



AFRL-PR-WP-TP-2007-232

**THE EFFECTS OF SPACE CHARGE IN A HYPERSONIC
MAGNETOHYDRODYNAMIC POWER GENERATOR**

Rene J. Thibodeaux

**Electrical Technology and Plasma Physics Branch
Power Division**

JUNE 2007

Approved for public release; distribution is unlimited.

See additional restrictions described on inside pages

STINFO COPY

**AIR FORCE RESEARCH LABORATORY
PROPULSION DIRECTORATE
WRIGHT-PATTERSON AIR FORCE BASE, OH 45433-7251
AIR FORCE MATERIEL COMMAND
UNITED STATES AIR FORCE**

REPORT DOCUMENTATION PAGE

Form Approved
OMB No. 0704-0188

The public reporting burden for this collection of information is estimated to average 1 hour per response, including the time for reviewing instructions, searching existing data sources, gathering and maintaining the data needed, and completing and reviewing the collection of information. Send comments regarding this burden estimate or any other aspect of this collection of information, including suggestions for reducing this burden, to Department of Defense, Washington Headquarters Services, Directorate for Information Operations and Reports (0704-0188), 1215 Jefferson Davis Highway, Suite 1204, Arlington, VA 22202-4302. Respondents should be aware that notwithstanding any other provision of law, no person shall be subject to any penalty for failing to comply with a collection of information if it does not display a currently valid OMB control number. **PLEASE DO NOT RETURN YOUR FORM TO THE ABOVE ADDRESS.**

1. REPORT DATE (DD-MM-YY) June 2007	2. REPORT TYPE Conference Paper Postprint	3. DATES COVERED (From - To) 07 November 2006 – 13 June 2007
---	---	--

4. TITLE AND SUBTITLE THE EFFECTS OF SPACE CHARGE IN A HYPERSONIC MAGNETOHYDRODYNAMIC POWER GENERATOR	5a. CONTRACT NUMBER In-House
	5b. GRANT NUMBER
	5c. PROGRAM ELEMENT NUMBER 62203F

6. AUTHOR(S) Rene J. Thibodeaux	5d. PROJECT NUMBER 3145
	5e. TASK NUMBER 29
	5f. WORK UNIT NUMBER 314529M3

7. PERFORMING ORGANIZATION NAME(S) AND ADDRESS(ES) Electrical Technology and Plasma Physics Branch, Power Division Air Force Research Laboratory, Propulsion Directorate Wright-Patterson Air Force Base, OH 45433-7251 Air Force Materiel Command United States Air Force	8. PERFORMING ORGANIZATION REPORT NUMBER AFRL-PR-WP-TP-2007-232
--	---

9. SPONSORING/MONITORING AGENCY NAME(S) AND ADDRESS(ES) Air Force Research Laboratory Propulsion Directorate Wright-Patterson Air Force Base, OH 45433-7251 Air Force Materiel Command United States Air Force	10. SPONSORING/MONITORING AGENCY ACRONYM(S) AFRL/PRPE
	11. SPONSORING/MONITORING AGENCY REPORT NUMBER(S) AFRL-PR-WP-TP-2007-232

12. DISTRIBUTION/AVAILABILITY STATEMENT
Approved for public release; distribution is unlimited.

13. SUPPLEMENTARY NOTES
Presented at the 37th AIAA Plasmadynamics and Laser Conference, 16th International Conference on Magnetohydrodynamics, Miami, FL, 25 June 2007. PAO Case Number: AFRL/WS 07-1254, 29 May 2007. This is a work of the U.S. Government and is not subject to copyright protection in the United States. This paper contains color.

14. ABSTRACT
This paper explores a new MHD generator design that uses space charge to create an axial-symmetric electric field in the region between concentric cylindrical channels. The space charge fraction is shown to have a significant effect in the current density, power density, electric field, output voltage, efficiency, pressure drop, and enthalpy. The radial symmetry produces simple analytic solutions for these equations over a wide range of gas flow speeds. Adjustments in the space charge can be used to regulate the output voltage of the generator for a constant magnetic field. This technique can eliminate the need for a full output power conditioner.

15. SUBJECT TERMS
Magnetohydrodynamic Generator, Space Charge, Hypersonics, Scramjet

16. SECURITY CLASSIFICATION OF:			17. LIMITATION OF ABSTRACT: SAR	18. NUMBER OF PAGES 38	19a. NAME OF RESPONSIBLE PERSON (Monitor) Rene J. Thibodeaux
a. REPORT Unclassified	b. ABSTRACT Unclassified	c. THIS PAGE Unclassified			

The Effects of Space Charge in a Hypersonic Magnetohydrodynamic Power Generator

Rene J. Thibodeaux*

Air Force Research Laboratory, Wright-Patterson AFB Dayton, Ohio, 45433-7251

This paper will explore a new MHD generator design that uses space charge to create an axial-symmetric electric field in the region between concentric cylindrical channels. The space charge fraction is shown to have a significant effect in the current density, power density, electric field, output voltage, efficiency, pressure drop, enthalpy, and electromagnetic Reynolds number of the generator. The radial symmetry produces simple analytic solutions for these equations over a wide range of gas flow speeds. Adjustments in the space charge can be used to regulate the output voltage of the generator for a constant magnetic field. This technique can eliminate the need for a massive full output power conditioner. Space charging current (electron beams or corona ionization) is calculated. Also the space charging energy is used to plot the system weight benefit of using space charge voltage regulation versus voltage regulation using full output power conditioning. Plots of the generator output voltage, electric field, efficiency, and electromagnetic Reynolds number are also presented.

Nomenclature

J	=	current density
U	=	gas flow velocity
E	=	electric field
B	=	magnetic field
I	=	current
σ	=	conductivity
ρ	=	charge density
K_e	=	electron mobility
K_i	=	electron mobility
K	=	load factor
ν	=	collision frequency
α	=	electron density fraction – {electrons/cm ³ }/ {molecules/cm ³ }
β	=	positive ion density fraction – {positive ions/cm ³ }/ {molecules/cm ³ }
χ	=	negative ion density fraction – {negative ions/cm ³ }/ {molecules/cm ³ }
δ	=	space charge fraction (with positive ions only) $\delta = (\alpha - \beta)/\alpha$
Δ	=	space charge fraction (with negative and positive ions) $\Delta = (\alpha + \chi - \beta)/\alpha$

I. Introduction

MAGNETOHYDRODYNAMICS has been well demonstrated in large scale supersonic laboratory demonstrations since the 1950's. Small scale shock tube and wind tunnel experiments to investigate hypersonic MHD phenomena has also been the performed since 1950's, with the most recent well known work focused on the Russian of the "Ajax" vehicle concept first revealed in the 1990's. The Air Force Research Laboratory (AFRL)/Propulsion Directorate initiated the Hypersonic Vehicle Electric Power Systems (HVEPS) program in 2001 to investigate the realistic operation of MHD channels at hypersonic gas flow speeds and temperatures equivalent to scramjet engine conditions lasting for durations of several seconds. Development of this technology could make air-breathing MHD auxiliary power systems available for hypersonic vehicles for a wide

* HVEPS Program Manager, Propulsion Directorate, Power Division, Electrical Technology and Plasma Physics Branch, Member AIAA

variety of high power applications. Results of these tests would conclusively answer whether or not scramjets could directly power MHD generators. The test rig's mass flow rate was the known limiting factor in the output power of the generator. The major unknown was the non-uniformities in the plasma caused by the hypersonic gas flow.

HVEPS was a collaborative effort between General Atomics (GA), LyTec LLC, Pratt & Whitney Rocketdyne (PWR), United Technologies Research Center (UTRC), and NASA. The HVEPS program studied the feasibility of using MHD generators as electrical power sources; thereby overcoming the limitation in scramjets which lack rotating shafts in the direct gas flow and therefore can not directly power conventional rotating generators. The UTRC test was one of the final tasks of HVEPS which has include vehicle system studies, magnet and generator designs. This testing effort was performed at the UTRC Jet Burner Test Facility, Hartford, Connecticut. The test setup consisted of the scramjet combustor coupled with the MHD generator in the exhaust stream. The MHD generator was a constant cross-section rectangular geometry with a conventional diagonal electrode lined channel. For this demonstration, the system used a helium cooled superconducting magnet (3 Tesla capability) supplied by NASA/Marshall Space Flight Center. The combustion fuel was ethylene mixed with NaK seeding and oxygen to raise the combustion temperature above 4000 Rankine for sufficient electrical conductivity.

The goal of the tests was simply to measure the voltage/current during a 4 second burst created when the seeding released. Power was produced immediately every time seeding was applied to the combustor in 6 test runs made over the two separate days of testing, giving a high confidence that the test results are reproducible. The test results were used to map the power curves for various electrical load levels. The voltages varied from 100-400 VDC and the power levels ranged from 2-15 kW depending on loading. The real power levels were limited by the test rig mass flow rate, instantaneous electrical conductivity of gas, and the magnetic field.



Figure 1 HVEPS Scramjet Driven MHD Generator with Helium Cooled Magnet

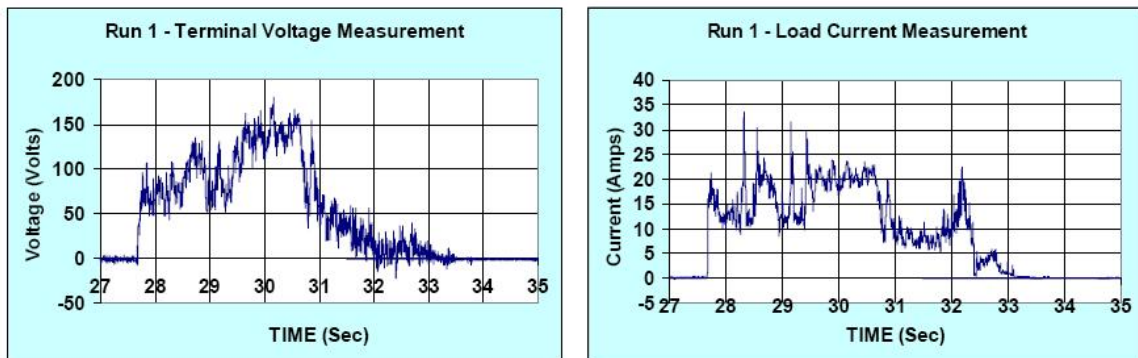


Figure 2 Voltage and Current Measurement from HVEPS Scramjet/MHD Generator

The system benefit of applying MHD to a hypersonic vehicle is easy to see when we compare the best representative of a real hypersonic vehicle power system: the Shuttle orbiter. The Shuttle uses fuel cells and hydrazine powered auxiliary power units for electrical and hydraulic power. The three fuel cells of the Shuttle are capable of a maximum continuous output of 21 kilowatts with 15-minute peaks of 36 kilowatts with a 255 lbs

package. The typical average power consumption of the orbiter is 14 kilowatts (7 kilowatts are available for payloads). The hydrazine APU's provide the hydraulic power for Shuttle Orbiter during the ascent, descent, and landing. The APU's power the aero control surfaces; engine thrust vector control, engine valves, landing gear, brakes, and steering. The APU's typically operate for 90 minutes over a power range of 6 kW to 110 kW. Proposals for an electrical APU replacement estimate the units would weight 80 lbs. If fuel cells were used instead, the peak 110 kilowatts for the equivalent replacement electrical actuators in the orbiter would require 1275 lbs of fuel cell to provide the total potential electrical power in the entire vehicle. The initial studies of HVEPS show that an MHD generator system (magnet, channel, seeding) can produce a 10 megawatt burst for 10 minutes in a package of less than 4000 lbs where the equivalent weight for a Shuttle APU would be 7000 lbs and for fuel cells would be 121000 lbs. Add to these weights, auxiliary power units would require heavy amounts of hydrazine and the fuel cells require heavy amounts of oxidizer to operate. Because the MHD generators extract power directly from scramjet flow, they generate the electrical voltage and current as soon as the seeding is added to the flow stream, in near instantaneous response times of milliseconds, ideal for many directed energy weapons.

Any attempt to use the extremely high speed gas flows to power a turbine would either directly destroy the internal turbine blades in the extreme heat of the inlet gas or would require an unacceptably enormous cooling system to prevent damage. MHD generators work optimally at the high temperatures of hypersonic flight. Studies have shown that hypersonic vehicle will likely require power levels into 100's kilowatts (possibly even megawatts) of power for aero control surface electrical actuators given the need for more maneuverability over flight durations of several hours. MHD generators can directly power the electrical actuators or can be applied to a magnetogasdynamic (MGD) "virtual control surface" to deflect the natural plasma surrounding the hypersonic vehicle. The natural (or microwave induced) plasmas can be channeled through a MGD "virtual cowl" at the scramjet inlet to increase inlet flow. In addition, startup of the scramjet may require a plasma torch to initiate combustion. Finally, a high power generator would make hypersonic aircraft strong candidates for directed energy weapons. The final test effort of this program is verification of a MHD computational fluid dynamic computer code that has been developed by Purdue University and the University of Tennessee Space Institute.

II. Technical and Historical Background of MHD

MHD generators produce a current in an ionized gas by passing the gas through a magnetic field. The magnetic electric field ($U \times B$) consists of a perpendicular (Faraday) component and an axial (Hall) component relative to the direction of motion. Electrons moving because of this field first form surface charges at of the MHD channel and develop an opposing electric field. Electrodes are positioned to use the Faraday or Hall fields, but diagonally connected electrodes generally produce the optimum configuration in rectangular channels by taking full advantage of both the Faraday and Hall electric fields simultaneously. The majority of MHD research has been with diagonally connected generators, although some pulse power generators utilized continuous Faraday electrode designs.



Figure 3 Combustion MHD Generator

Michael Faraday proposed the initial concepts of MHD in the 1830's. The first demonstration of an electric motor was based on a conducting wire rotating in the bath of liquid mercury and was actually a demonstration of MHD. Concepts for electrically conducting gas MHD generators began to appear in patents as early as 1910; however, no methods of ionization were suggested, so actual devices were never built. The first working experiments on a conducting gas MHD generator began with Karlovitz and Halasz in 1938 at Westinghouse. This generator was a coaxial cylindrical design, but with limited capability as the basic plasma physics was not well understood at that time. As more accurate plasma physics models were applied, more practical generators were constructed in the 1960's and 1970's. MHD aerodynamic controls were design by Krantowitz in 1955 with the use of MHD for reactive control of re-entry vehicles using high natural thermal ionization produced from the re-entry drag at hypersonic speeds. A large Air Force MHD research program in the 1960's and 1970's focused on supersonic combustor flows and several studies used turbine engine exhaust flows.

The combustion-driven MHD power generation is the most mature and well understood type of MHD technology application. Combustion driven generators need internal oxidizers, which can be a disadvantage for any long duration aerospace mission. Combustion MHD is, however, competitive with almost any energy storage and rotating generators over durations of 1 to 1000 seconds. MHD pulse power systems with power density on the order 100^3 MW/m³ have been well demonstrated as practical systems over the pass 40 years. Russian work in 1980's was reported to have produced an output of 500 MW at a power density approximately 600 MW/m³. The theoretical power densities of hypersonic MHD generators can be made extremely high (100's to 1000's MW/m³). No other non-nuclear power technology can compete with this technology for hypersonic air and space vehicle power sources.

Thermal ionization is a byproduct of the high collision rate of the atoms in the high temperature gas. Achieving natural thermal ionization in molecular gases requires extremely high temperature. For example, ionization of pure air requires temperatures over 4,000 °K. The traditional technique of adding high electron affinity alkali metals is easier in the high temperature flow. Additional ionization using high electric fields coronas, electron beams, or high power microwaves is possible; the practical limitation in any case is the power is required.

Large vehicle scramjet engines will need to produce gigawatts of power to accelerate and reach a constant cruise speed, and will need to produce hundreds of megawatts of power to maintain cruise speeds. MHD generators can easily extract large amounts of electric power from the tremendous kinetic and thermal energy available in a hypersonic flow. Demonstrated enthalpy extraction of MHD generators in the 0.5-2.0 MW range have been at the order of 1.0-5.0 % and for larger units in the 10-500 MW range, enthalpy extraction increases to the 10.0-20.0 % range. For large-scale MHD power systems, isentropic efficiency approaching 80% is theoretically possible. Since scramjets are non-rotating machines, non-rotating MHD generators are a natural match to produce efficient power.

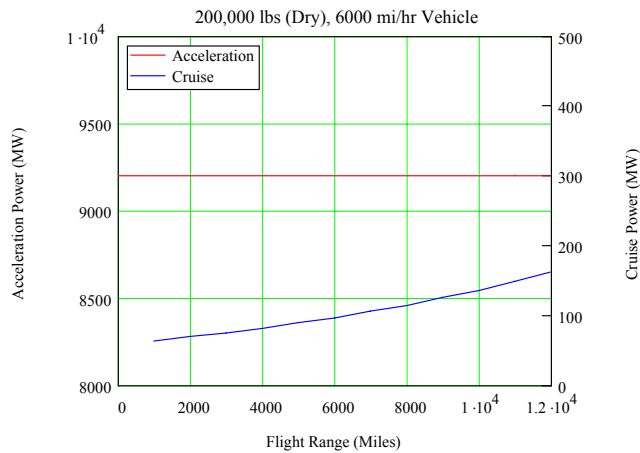


Figure 5 Hypersonic Vehicle Engine Power

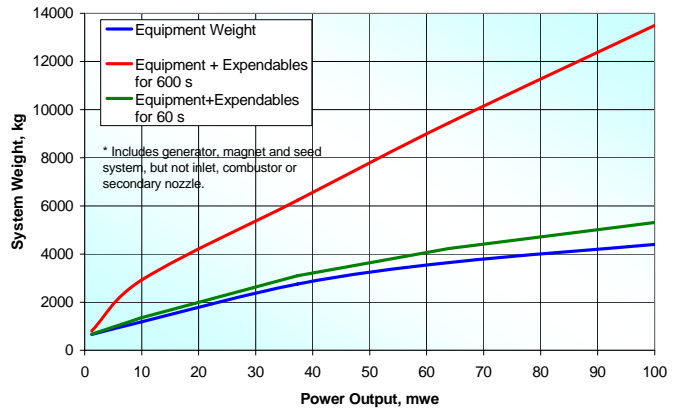


Figure 4 MHD Power System Weight Estimate

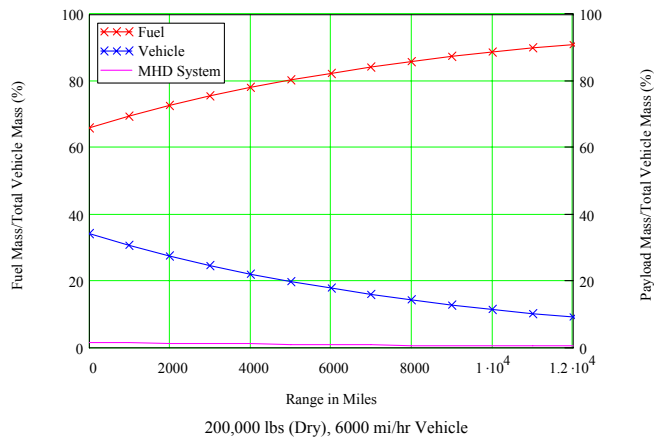


Figure 6 Hypersonic Vehicle Mass Fractions

The high-speed gas flow produces extremely high power density MHD power systems that are a small percentage of the total vehicle weight (4000 kg power system/100,000 kg vehicle = 4%). This weight is achievable even with helium cooled superconductor magnets; high temperature YBCO superconductor magnets have the potential of using lightweight liquid nitrogen (or liquid hydrogen) temperature cryocoolers.

III. Space Charge Voltage Regulation Concept

The measurements show in Fig. 2 show that the actual voltage and current measurements from a MHD generator would require significant filtering to produce a smooth output. In addition, the voltage is directly determined by the gas flow velocity because the electric field in the generator is $U \times B$ where U is the flow velocity and B the magnetic field. As U varies, the only alternatives to regulate the output voltage are adjust the magnet current to change the magnetic field or perform full output power conditioning with heavy capacitor filtering. A generally ignored factor is that the current is a combination of the conductivity and space charge as which can be written as $J = \sigma(E + U \times B) + \rho U$, where J is the current density, σ is the conductivity, E the electric field, U the gas flow velocity, B the magnetic field, and ρ is the space charge density. The electric fields from space charge in a rectangular channel tend to produce high electric fields in the sharp corners of the channel. Because the magnetic field across the channel also creates basically a transverse electric, the radial electric fields from space charge will disturb the magnet's electric field in certain regions, so space charge is neutralized as much as possible in a rectangular MHD generator to minimize this effect.

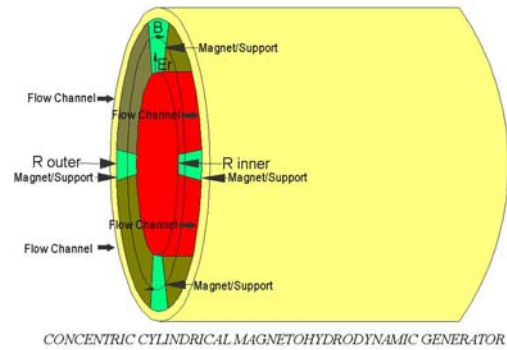


Figure 7 Conceptual Cylindrical MHD Generator

The symmetry of the space charge's electric field as calculated by Gauss's law indicates that a symmetric geometry such as a cylinder or sphere can take advantage of the space charge electric. This in fact was the physical basis for the performance of electron tubes as show in Fig 4 above where electrons are the actual space charge. The triode in fact introduces a control grid to regulate the voltage between the cathode and anode. The electric field is easily calculated for a cylindrical geometry with an enclosed charge using Gauss's Law. In the case of MHD channel with space charge, the enclosed charge is assumed distributed uniformly in a long cylindrical geometry to produce primarily a radial electric field (the end effects of the field are assumed to be negligible). The radial electric field of the space charge aligns with the radial electric field created from the circular magnetic field.

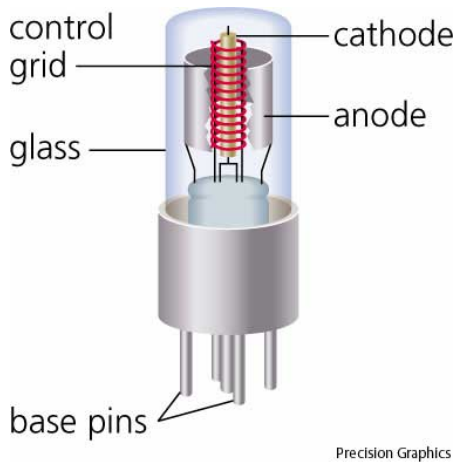


Figure 8 Concentric Electrodes in Triode

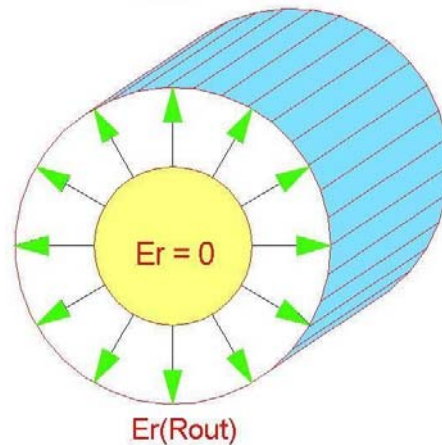


Figure 9 Radial Electric Field in a Cylindrical Channel

IV. Theoretical Analysis of Space Charge Effects

A. Generator Output Voltage and Electric Field

We will now derive the equations and plots that show the effects of space charge on the output voltage, electrode electric field, magnetic field, electrical efficiency, generator pressure drop, and extracted enthalpy. The calculations will demonstrate that adjusting the space charge is a reasonable means to regulate the output voltage (electric field) and reduce the magnetic field required for a particular power level. For the plot calculations, the generator power level is set at 5 megawatts and the generator dimensions are $R_{\text{outer}} = 1$ m, $R_{\text{inner}} = 0.9$ m, $L = 1$ m, (the resulting power density is $P_d = 8.4$ MW/m³). Assume the propulsion is provided by a hydrocarbon fueled scramjet. Kerosene and oxygen give a reasonable representation of the electron-molecular collision cross-section (approximately $Q_e = 40 \times 10^{-20}$ m²) for a hydrocarbon, and if the combustion temperature is about $T_{\text{in}} = 3000$ °K, the electron mobility works out to be $K_e = 0.528$ m/s/V/m. We will assume the electron density is sufficient to yield an electron conductivity $\sigma_e = -20$ mhos. The minus sign is used in the electron conductivity to calculate the correct signs and values for voltage and electric field because the space charge fraction must be $\delta < 0$ for a plasma dominated by electrons and negative ions. The inlet gas pressure is set at $P_{\text{inlet}} = 1$ atm and the true Mach numbers are determined using the temperature dependent speed of sound, $C_m := \sqrt{\gamma \cdot R_g \cdot T_{\text{in}}}$, where the Universal gas constant for air is $R_g(\text{air}) = 287.05$ Joule/Kg/°K, and the constant pressure specific heat is $C_p(\text{air}) = 1005$ J/Kg/K and the ratio of specific heat is $\gamma = 1.4$.

The complete current density is determined by Ohm's Law with the Hall current and space charge terms,

$$\vec{J} = \sigma_{ij} \cdot \left(\vec{E} + \vec{U} \times \vec{B} + \frac{1}{\rho} \cdot \vec{J} \times \vec{B} \right) + \rho \cdot \vec{U} \quad (1)$$

where the current density, electric field, magnetic field, and flow velocity vectors are in cylindrical coordinates,

$$\vec{J} = \begin{pmatrix} J_r \\ J_\theta \\ J_z \end{pmatrix} \quad \vec{E} = \begin{pmatrix} E_r \\ 0 \\ E_z \end{pmatrix} \quad \vec{U} = \begin{pmatrix} 0 \\ 0 \\ U_z \end{pmatrix} \quad \vec{B} = \begin{pmatrix} 0 \\ B_\theta \\ 0 \end{pmatrix} \quad (2)$$

The magnetic field B_θ between concentric cylinders with inner radius R_{inner} and outer radius R_{outer} ,

$$B_\theta(r) = \frac{\mu_0 \cdot N \cdot I}{2 \cdot \pi \cdot r} \quad (3)$$

The maximum magnetic field occurs at R_{inner}

$$B_m = \frac{\mu_0 \cdot N \cdot I}{2 \cdot \pi \cdot R_{\text{in}}} \quad (4)$$

The internal magnetic field can be defined with the maximum magnetic field,

$$B_\theta(r) = B_m \cdot \frac{R_{\text{in}}}{r} \quad (5)$$

Conductivity tensor for electrons (or ions) is

$$\sigma_{ij} = \begin{bmatrix} \frac{\sigma}{1 + (K \cdot B_\theta)^2} & 0 & \frac{-\sigma \cdot (K \cdot B_\theta)}{1 + (K \cdot B_\theta)^2} \\ 0 & \sigma & 0 \\ \frac{\sigma \cdot (K \cdot B_\theta)}{1 + (K \cdot B_\theta)^2} & 0 & \frac{\sigma}{1 + (K \cdot B_\theta)^2} \end{bmatrix} \quad (6)$$

The conductivity is the product of mobility and charge density, $\sigma_e = K_e \cdot \rho_e$ and $\sigma_i = K_i \cdot \rho_i$. The total current density,

$$\vec{J} = (\sigma_{ij} - \sigma_{eij}) \cdot (\vec{E} + \vec{U} \times \vec{B}) + \left(\frac{\sigma_{ij}}{\rho_i} - \frac{\sigma_{eij}}{\rho_e} \right) \cdot (\vec{J} \times \vec{B}) + (\rho_i - \rho_e) \cdot \vec{U} \quad (7)$$

The electron mobility (K_e) and the ion mobility (K_i) from the electron collision frequency (ν_e) and ion collision frequency (ν_i) are determined by,

$$K_e = \frac{e}{m_e} \cdot \frac{1}{\nu_e} \quad (8)$$

$$K_i = Z \cdot \frac{e}{m_i} \cdot \frac{1}{\nu_i}$$

Where the electron charge is $e = 1.60217733 \cdot 10^{-19}$ coulombs and the electron mass is $m_e = 9.1093897 \cdot 10^{-31}$ kg. The ion mass is $m_i = A \cdot \text{AMU}$ where A is the atomic weight and $\text{AMU} = 1.6605402 \cdot 10^{-27}$ kg (Atomic Mass Unit) and the ion charge number (or the electrons removed) is Z . The electron collision frequency (ν_e) and the ion collision frequency (ν_i) are related to the electron-molecular and ion-molecular collision cross-sections (Q_e, Q_i),

$$\nu_e = n_0 \cdot Q_e \cdot \sqrt{\frac{8 \cdot k \cdot T_{in}}{\pi \cdot m_e}} \quad (9)$$

$$\nu_i = n_0 \cdot Q_i \cdot \sqrt{\frac{16 \cdot k \cdot T_{in}}{\pi \cdot m_i}}$$

where the gas density is $n_0 = P_{inlet}/k \cdot T_{inlet}$ or the ideal gas law at inlet temperature and gas pressure (Boltzman constant $k = 1.380658 \cdot 10^{-23}$ J/K). The electron mobility,

$$K_e = \frac{e}{m_e} \cdot \frac{1}{n_0 \cdot Q_e \cdot \sqrt{\frac{8 \cdot k \cdot T_{in}}{\pi \cdot m_e}}} = \frac{e}{m_e} \cdot \frac{1}{\frac{P_{in}}{k \cdot T_{in}} \cdot Q_e \cdot \sqrt{\frac{8 \cdot k \cdot T_{in}}{\pi \cdot m_e}}} \quad (10)$$

The ion mobility

$$K_i = Z \cdot \frac{e}{m_i} \cdot \frac{1}{n_0 \cdot Q_i \cdot \sqrt{\frac{16 \cdot k \cdot T_{in}}{\pi \cdot m_i}}} = Z \cdot \frac{e}{m_i} \cdot \frac{1}{\frac{P_{in}}{k \cdot T_{in}} \cdot Q_i \cdot \sqrt{\frac{16 \cdot k \cdot T_{in}}{\pi \cdot m_i}}} \quad (11)$$

The ratio of electron mobility to ion mobility is $60.38(Q_i/Q_e)A^{1/2}$ and since $Q_i \gg Q_e$, the electron mobility is substantially larger than any ion mobility ($K_e \gg K_i$). The greater mobility of the electron allows the current density to be accurately approximated (in matrix form),

$$\begin{pmatrix} J_r \\ J_\theta \\ J_z \end{pmatrix} = \begin{bmatrix} 1 & 0 & -K_e \cdot B\theta \\ 1 + (K_e \cdot B\theta)^2 & 1 + (K_e \cdot B\theta)^2 & 0 \\ 0 & 1 & 0 \\ K_e \cdot B\theta & 0 & 1 \\ 1 + (K_e \cdot B\theta)^2 & 1 + (K_e \cdot B\theta)^2 & 0 \end{bmatrix} \cdot \left[-\sigma_e \cdot \begin{pmatrix} E_r \\ 0 \\ E_z \end{pmatrix} + \begin{pmatrix} 0 \\ 0 \\ U_z \end{pmatrix} \times \begin{pmatrix} 0 \\ B\theta \\ 0 \end{pmatrix} \right] - K_e \cdot \begin{pmatrix} J_r \\ J_\theta \\ J_z \end{pmatrix} \times \begin{pmatrix} 0 \\ B\theta \\ 0 \end{pmatrix} + \left(\frac{\sigma_i}{K_i} - \frac{\sigma_e}{K_e} \right) \cdot \begin{pmatrix} 0 \\ 0 \\ U_z \end{pmatrix} \quad (12)$$

The space charge term is

$$\rho_i - \rho_e = \frac{\sigma_i}{K_i} - \frac{\sigma_e}{K_e} \quad (13)$$

The neutral charged plasma condition is $\rho_i - \rho_e = 0$, and the ionized plasma conditions are $\rho_e > \rho_i$ (net negative space charge) and $\rho_e < \rho_i$ (net positive space charge). The space charge densities can be expressed as a fraction of

the gas density n_0 , $\alpha \cdot e \cdot n_0 = \rho_e$ (positive ion fraction - α), $\beta \cdot e \cdot n_0 = \rho_i$ (electron fraction - β), $\chi \cdot e \cdot n_0 = \rho_n$ (negative ion fraction - χ). The net space charge becomes,

$$\rho_i - \rho_e = \alpha \cdot e \cdot n_0 - \beta \cdot e \cdot n_0 = (\alpha - \beta) \cdot e \cdot n_0 = \frac{\alpha - \beta}{\beta} \cdot \rho_e = \delta \cdot \frac{\sigma_e}{K_e} \quad (14)$$

where $\delta = (\alpha - \beta)/\alpha$ is the relative excess fraction of electron charge. The plasma created by thermal ionization is a loosely bound cloud of electrons and ions which appear from the outside to be neutral. A net space charge of electrons can be added externally to the plasma by an electron beam and a net space charge of negative ions can be added by a negative corona. A complete mixture of free electrons (α), positive ions (β), and negative ions (χ) can be described by a similar term, Δ ,

$$\rho_i - \rho_n - \rho_e = (\alpha - \gamma - \beta) \cdot e \cdot n_0 = \frac{\alpha - \gamma - \beta}{\beta} \cdot \rho_e = \Delta \cdot \frac{\sigma_e}{K_e} \quad (15)$$

where $\Delta = (\alpha + \chi - \beta)/\alpha$ is the excess fraction of electron charge (with negative and positive ion). The possible charge conditions are: neutral space charge $\delta = 0$ or $\Delta = 0$; negative space charge $\delta > 0$ or $\Delta > 0$; positive space charge $\delta < 0$ or $\Delta < 0$.

The electron dominated approximation for total current density using the excess charge term (δ),

$$\begin{pmatrix} J_r \\ J_\theta \\ J_z \end{pmatrix} = \begin{bmatrix} \frac{1}{1 + (K_e \cdot B\theta)^2} & 0 & \frac{-K_e \cdot B\theta}{1 + (K_e \cdot B\theta)^2} \\ 0 & 1 & 0 \\ \frac{K_e \cdot B\theta}{1 + (K_e \cdot B\theta)^2} & 0 & \frac{1}{1 + (K_e \cdot B\theta)^2} \end{bmatrix} \cdot \left[-\sigma_e \cdot \begin{pmatrix} E_r \\ 0 \\ E_z \end{pmatrix} + \begin{pmatrix} 0 \\ 0 \\ U_z \end{pmatrix} \times \begin{pmatrix} 0 \\ B\theta \\ 0 \end{pmatrix} - K_e \cdot \begin{pmatrix} J_r \\ J_\theta \\ J_z \end{pmatrix} \times \begin{pmatrix} 0 \\ B\theta \\ 0 \end{pmatrix} \right] + \left(\delta \cdot \frac{\sigma_e}{K_e} \right) \cdot \begin{pmatrix} 0 \\ 0 \\ U_z \end{pmatrix} \quad (16)$$

In matrix form, the current density is,

$$\begin{pmatrix} J_r \\ J_\theta \\ J_z \end{pmatrix} = \begin{bmatrix} [(1 + \delta) \cdot U_z \cdot B\theta - E_r] \cdot \sigma_e \\ 0 \\ (U_z \delta - K_e \cdot E_z) \cdot \frac{\sigma_e}{K_e} \end{bmatrix} \quad (17)$$

The three load connections possible are the transverse Faraday load ($E_z = 0$), the axial Hall load ($E_r = 0$) and the diagonal load (non zero E_z and E_r). For a Faraday connection, the axial electric field is $E_z = 0$,

$$\begin{pmatrix} J_r \\ J_\theta \\ J_z \end{pmatrix} = \begin{bmatrix} [(1 + \delta) \cdot U_z \cdot B\theta - E_r] \cdot \sigma_e \\ 0 \\ (U_z \delta) \cdot \frac{\sigma_e}{K_e} \end{bmatrix} \quad (18)$$

The power density is determined using the total electric field applied to the electrons,

$$\vec{P}_d = \vec{J} \cdot (\vec{E} + \vec{U} \times \vec{B}) = \begin{bmatrix} [(1 + \delta) \cdot U_z \cdot B\theta - E_r] \cdot \sigma_e \\ 0 \\ (U_z \delta) \cdot \frac{\sigma_e}{K_e} \end{bmatrix} \cdot \left[\begin{pmatrix} E_r \\ 0 \\ 0 \end{pmatrix} + \begin{pmatrix} 0 \\ 0 \\ U_z \end{pmatrix} \times \begin{pmatrix} 0 \\ B\theta \\ 0 \end{pmatrix} \right] \quad (19)$$

Performing the multiplication

$$\vec{P}_d = -\sigma_e \cdot (U_z \cdot B\theta - E_r) \cdot [(1 + \delta) \cdot (U_z \cdot B\theta) - E_r] \quad (20)$$

This implies the minimum conductivity is,

$$\sigma_e = \frac{-Pd}{(B\theta \cdot U_z - E_r) \cdot [(1 + \delta) \cdot (U_z B\theta) - E_r]} \quad (21)$$

The Hall load generator current density becomes

$$\begin{pmatrix} J_r \\ J_\theta \\ J_z \end{pmatrix} = \begin{pmatrix} [(1 + \delta) \cdot U_z B\theta] \cdot \sigma_e \\ 0 \\ (U_z \delta - K_e \cdot E_z) \cdot \frac{\sigma_e}{K_e} \end{pmatrix} \quad (22)$$

The Hall generator electrical power density,

$$Pd = \begin{pmatrix} [(1 + \delta) \cdot U_z B\theta] \cdot \sigma_e \\ 0 \\ (U_z \delta - K_e \cdot E_z) \cdot \frac{\sigma_e}{K_e} \end{pmatrix} \cdot \left[\begin{pmatrix} 0 \\ 0 \\ E_z \end{pmatrix} + \begin{pmatrix} 0 \\ 0 \\ U_z \end{pmatrix} \times \begin{pmatrix} 0 \\ B\theta \\ 0 \end{pmatrix} \right] \quad (23)$$

Performing the multiplication,

$$Pd = -\sigma_e \cdot \left[(1 + \delta) \cdot (U_z B\theta)^2 + \left(1 - \delta \cdot \frac{U_z}{K_e \cdot E_z} \right) \cdot E_z^2 \right] \quad (24)$$

The diagonal generator current density (E_r and E_z are non-zero),

$$Pd = \vec{J} \cdot \vec{E} = \begin{pmatrix} [(1 + \delta) \cdot U_z B\theta - E_r] \cdot \sigma_e \\ 0 \\ (U_z \delta - K_e \cdot E_z) \cdot \frac{\sigma_e}{K_e} \end{pmatrix} \cdot \left[\begin{pmatrix} E_r \\ 0 \\ E_z \end{pmatrix} + \begin{pmatrix} 0 \\ 0 \\ U_z \end{pmatrix} \times \begin{pmatrix} 0 \\ B\theta \\ 0 \end{pmatrix} \right] \quad (25)$$

Performing the multiplication

$$Pd = -\sigma_e \cdot \left[\left[1 - (2 + \delta) \cdot \frac{U_z B\theta}{E_r} \right] \cdot E_r^2 + (1 + \delta) \cdot (U_z B\theta)^2 + \left(1 - \delta \cdot \frac{U_z}{K_e \cdot E_z} \right) \cdot E_z^2 \right] \quad (26)$$

The total radial electric field E_r is the sum of the fields produced by the surface charge of the electrodes, the space charge, and the magnetically induced electric field

$$E(r) = E_s(r) + E_p(r) + EB(r) \quad (27)$$

The induced electric field from the magnetic field $B_\theta(r) = B_m (R_{inner}/r)$

$$EB(r) = U_z B\theta(r) = U_z B_m \frac{R_{in}}{r} \quad (28)$$

The magnet's electrical potential is determined from the its electric field

$$\frac{d}{dr} VB = EB(r) \quad (29)$$

Integrating from the inner radius to some point inside

$$VB(r) = \int_{R_{in}}^r U_z B_m \frac{R_{in}}{R} dR \quad (30)$$

Using the change of variable $X = r/R_{\text{inner}}$, $r = R_{\text{inner}}X$, $dr = R_{\text{inner}}dX$,

$$VB(r) = \int_1^{Xr} U_z B_m \frac{R_{\text{in}}}{X} dX \quad (31)$$

The potential from the magnetic field

$$VB(r) = U_z B_m R_{\text{in}} \ln\left(\frac{r}{R_{\text{in}}}\right) \quad (32)$$

Integrating from the inner radius to a point inside

$$VB(R_{\text{out}}) = U_z B_m R_{\text{in}} \ln\left(\frac{R_{\text{out}}}{R_{\text{in}}}\right) \quad (33)$$

The electric field from the electrode's surface charge in a classic rectangular MHD channel is a constant value and so the potential is a simple function $V_s = x E_s$, where E_s is the surface charge electric field and x is the width of the channel. Since the surface charge is induced by the magnet electric field, the electrode electric field is usually defined by a proportional constant K called the "load factor" so that $E_s = K E_b$. This is unique to the rectangular geometry since load factor is correctly defined by the surface charge potential and the magnet's electric potential ($V_s = K V_b$). The "load factor" is a more complicated concept in a cylindrical geometry since any voltage is dependent on geometry, so that load factor must be defined for at a specific location.

We now calculate the space charge potential from Gauss's law. The electrode surface charge density Σ over an electrode surface area (radius R_{in} and length L_{elec}) acts like a space charge ρ_s

$$\rho_s = \Sigma \cdot \frac{2 \cdot \pi \cdot R_{\text{in}} \cdot L_{\text{elec}}}{\pi R_{\text{in}}^2 \cdot L_{\text{elec}}} = \Sigma \cdot \frac{2}{R_{\text{in}}} \quad (34)$$

The potential from the surface charge is determined from Poisson's equation (or equivalently Gauss's law)

$$\frac{1}{r} \cdot \frac{d}{dr} \left(r \cdot \frac{d}{dr} V_s(r) \right) = 2 \cdot \frac{\Sigma}{R_{\text{in}} \cdot \epsilon_0} \quad (35)$$

Transposing rdr ,

$$d \left(r \cdot \frac{d}{dr} V_s(r) \right) = 2 \cdot \frac{\Sigma}{\epsilon_0} \cdot \frac{r}{R_{\text{in}}} \cdot dr \quad (36)$$

Integrating from r to R_{in} ,

$$r \cdot \frac{d}{dr} V_s(r) = \int_{R_{\text{in}}}^r \left(2 \cdot \frac{\Sigma}{\epsilon_0} \right) \cdot \frac{R}{R_{\text{in}}} dR = \frac{r^2}{R_{\text{in}}} \cdot \frac{\Sigma}{\epsilon_0} - R_{\text{in}} \cdot \frac{\Sigma}{\epsilon_0} \quad (37)$$

Dividing by r ,

$$\frac{d}{dr} V_s(r) = \left(\frac{r}{R_{\text{in}}} - \frac{R_{\text{in}}}{r} \right) \cdot \frac{\Sigma}{\epsilon_0} \quad (38)$$

The surface charge potential becomes

$$V_s(r) = \int_{R_{\text{in}}}^r \left(\frac{R}{R_{\text{in}}} - \frac{R_{\text{in}}}{R} \right) \cdot \frac{\Sigma}{\epsilon_0} dR \quad (39)$$

Applying the change of variable $X = r/R_{inner}$, $r = R_{inner}X$, $dr = R_{inner}dX$,

$$V_s(r) = \int_1^{Xr} \left(X - \frac{1}{X} \right) \cdot \frac{\Sigma}{\epsilon_0} \cdot R_{in} dX \quad (40)$$

The integral becomes

$$V_s(r) = \left(Xr^2 - \ln(Xr) - 1 \right) \cdot \frac{\Sigma}{2} \cdot \frac{R_{in}}{\epsilon_0} \quad (41)$$

The result is the surface charge voltage inside the channel,

$$V_s(r) = \left[\left(\frac{r}{R_{in}} \right)^2 - \ln\left(\frac{r}{R_{in}} \right) - 1 \right] \cdot \frac{\Sigma}{2} \cdot \frac{R_{in}}{\epsilon_0} \quad (42)$$

The plasma's space charge potential is determined from Poisson's equation (Gauss' Law)

$$\frac{1}{r} \cdot \frac{d}{dr} \left[r \cdot \left(\frac{dV}{dr} \right) \right] + \frac{d}{dz} \frac{d}{dz} V = \frac{\rho_i - \rho_e}{\epsilon_0} = \frac{\delta}{\epsilon_0} \cdot \frac{\sigma_e}{Ke} \quad (43)$$

The axial electric field E_z is determined by

$$E_z = \frac{d}{dz} V \quad (44)$$

But for the Faraday generator $E_z = 0$

$$\frac{d}{dz} \frac{d}{dz} V = \frac{d}{dz} E_z = 0 \quad (45)$$

The space charge potential will be calculated for a uniform space charge to maintain simplicity,

$$\frac{1}{r} \cdot \frac{d}{dr} \left[r \cdot \left(\frac{dV_p(r)}{dr} \right) \right] = \frac{\delta}{\epsilon_0} \cdot \frac{\sigma_e}{Ke} \quad (46)$$

Transposing rdr

$$d \left[r \cdot \left(\frac{dV_p(r)}{dr} \right) \right] = \frac{\delta}{\epsilon_0} \cdot \frac{\sigma_e}{Ke} \cdot r \cdot dr \quad (47)$$

Integrating the equation over r to R_{in}

$$r \cdot \left(\frac{dV_p(r)}{dr} \right) = \frac{\delta}{\epsilon_0} \cdot \frac{\sigma_e}{Ke} \cdot \frac{r^2 - R_{in}^2}{2} \quad (48)$$

Dividing by r

$$\left(\frac{dV_p(r)}{dr} \right) = \frac{\delta}{2\epsilon_0} \cdot \frac{\sigma_e}{Ke} \cdot \left(r - \frac{R_{in}^2}{r} \right) \quad (49)$$

The integral can be rewritten as,

$$\int_{R_{in}}^{R_{out}} \frac{d}{dr} V_p(r) dr = \int_{R_{in}}^{R_{out}} \frac{\delta}{\epsilon_0} \cdot \frac{\sigma_e}{Ke} \cdot \frac{R_{in}}{2} \cdot \left(\frac{r}{R_{in}} - \frac{R_{in}}{r} \right) dr \quad (50)$$

Again we apply the change of variable $X = r/R_{\text{inner}}$ ($Xr = r/R_{\text{in}}$), $r = R_{\text{inner}}X$, $dr = R_{\text{inner}}dX$,

$$V_{\rho}(r) = \int_1^{Xr} \left(X - \frac{1}{X} \right) \cdot \frac{\delta}{\epsilon_0} \cdot \frac{\sigma_e}{K_e} \cdot \frac{R_{\text{in}}^2}{2} dX = \frac{1}{4} \cdot \left(\frac{\delta}{\epsilon_0} \cdot \frac{\sigma_e}{K_e} \right) \cdot R_{\text{in}}^2 \cdot \left(Xr^2 - 2 \cdot \ln(Xr) - 1 \right) \quad (51)$$

The space charge potential becomes

$$V_{\rho}(r) = \frac{1}{4} \cdot \left(\frac{\delta}{\epsilon_0} \cdot \frac{\sigma_e}{K_e} \right) \cdot R_{\text{in}}^2 \cdot \left[\left(\frac{r}{R_{\text{in}}} \right)^2 - 2 \cdot \ln \left(\frac{r}{R_{\text{in}}} \right) - 1 \right] \quad (52)$$

The total potential is the sum of the surface charge, space charge, and magnetic field potentials

$$V(r) = V_s(r) + V_{\rho}(r) + V_B(r) \quad (53)$$

Substituting the various potentials, the complete potential is,

$$V(r) = \left[\left(\frac{\Sigma}{2} \cdot \frac{R_{\text{in}}}{\epsilon_0} \right) + \frac{1}{4} \cdot \left(\frac{\delta}{\epsilon_0} \cdot \frac{\sigma_e}{K_e} \right) \cdot R_{\text{in}}^2 \right] \cdot \left[\left(\frac{r}{R_{\text{in}}} \right)^2 - 2 \cdot \ln \left(\frac{r}{R_{\text{in}}} \right) - 1 \right] + U_z B_m R_{\text{in}} \cdot \ln \left(\frac{r}{R_{\text{in}}} \right) \quad (54)$$

The total load voltage

$$V_{\text{load}} = \left[\left(\frac{\Sigma}{2} \cdot \frac{R_{\text{in}}}{\epsilon_0} \right) + \frac{1}{4} \cdot \left(\frac{\delta}{\epsilon_0} \cdot \frac{\sigma_e}{K_e} \right) \cdot R_{\text{in}}^2 \right] \cdot \left[\left(\frac{R_{\text{out}}}{R_{\text{in}}} \right)^2 - 2 \cdot \ln \left(\frac{R_{\text{out}}}{R_{\text{in}}} \right) - 1 \right] + U_z B_m R_{\text{in}} \cdot \ln \left(\frac{R_{\text{out}}}{R_{\text{in}}} \right) \quad (55)$$

From the total load voltage the induced surface charge on the inner electrode can be calculated

$$\Sigma = 2 \cdot \frac{\epsilon_0}{R_{\text{in}}} \cdot \left[\frac{V_{\text{load}} - U_z B_m R_{\text{in}} \cdot \ln \left(\frac{R_{\text{out}}}{R_{\text{in}}} \right)}{\left(\frac{R_{\text{out}}}{R_{\text{in}}} \right)^2 - 2 \cdot \ln \left(\frac{R_{\text{out}}}{R_{\text{in}}} \right) - 1} - \frac{1}{4} \cdot \left(\frac{\delta}{\epsilon_0} \cdot \frac{\sigma_e}{K_e} \right) \cdot R_{\text{in}}^2 \right] \quad (56)$$

The traditional “load factor” definition is $K = V_{\text{load}}/V_B(R_{\text{out}})$

$$K = \frac{\left(\frac{\Sigma}{2} \cdot \frac{R_{\text{in}}}{\epsilon_0} \right) + \frac{1}{4} \cdot \left(\frac{\delta}{\epsilon_0} \cdot \frac{\sigma_e}{K_e} \right) \cdot R_{\text{in}}^2}{U_z B_m R_{\text{in}} \cdot \ln \left(\frac{R_{\text{out}}}{R_{\text{in}}} \right)} \cdot \left[\left(\frac{R_{\text{out}}}{R_{\text{in}}} \right)^2 - 2 \cdot \ln \left(\frac{R_{\text{out}}}{R_{\text{in}}} \right) - 1 \right] + 1 \quad (57)$$

Load factor is now dependent on the space charge fraction as well as the ratio of $R_{\text{out}}/R_{\text{in}}$. The dependence on space charge factor means the load factor changes as space charge changes. We can apply a condition that if the voltage contributed by the surface charge is negligible compared to the voltage from the space charge, ($V_s \ll V_{\rho}$ which is the same as $\Sigma = 0$), then the internal voltage of the generator strictly becomes a function of the magnet’s electric field and the space charge of the plasma (the outer electrode surface charge does not contribute to the internal electric field because of Gauss’s Law). The condition that space charge voltage is greater than the surface charge voltage is,

$$1 > \frac{\left(\frac{\Sigma}{\epsilon_0} \cdot \frac{R_{\text{in}}}{2} \right)}{\left[\frac{1}{4} \cdot \left(\frac{\delta}{\epsilon_0} \cdot \frac{\sigma_e}{K_e} \right) \cdot R_{\text{in}}^2 \right]} \quad (58)$$

The lower limit of space charge fraction to maintain space charge voltage greater than surface charge voltage is,

$$\delta > \frac{V_{load} - U_z B_m R_{in} \ln\left(\frac{R_{out}}{R_{in}}\right)}{\left[\left(\frac{R_{out}}{R_{in}}\right)^2 - 2 \cdot \ln\left(\frac{R_{out}}{R_{in}}\right) - 1\right] \cdot \left[\frac{1}{2} \cdot \left(\frac{1}{\epsilon_0} \cdot \frac{\sigma_e}{K_e}\right) \cdot R_{in}^2\right]} \quad (59)$$

This becomes the dividing line between classic magnetohydrodynamics and electromagnetohydrodynamics, where the independent space charge electric field dominates the electrode surface charge electric field induced by the magnet's U X B electric field. Assuming the surface charge is negligible, $\Sigma = 0$,

$$V_{total}(r) = \frac{1}{4} \cdot \left(\frac{\delta}{\epsilon_0} \cdot \frac{\sigma_e}{K_e}\right) \cdot R_{in}^2 \cdot \left[\left(\frac{r}{R_{in}}\right)^2 - 2 \cdot \ln\left(\frac{r}{R_{in}}\right) - 1\right] + U_z B_m R_{in} \ln\left(\frac{r}{R_{in}}\right) \quad (60)$$

The load voltage at R_{out} ,

$$V_{load} = \frac{1}{4} \cdot \left(\frac{\delta}{\epsilon_0} \cdot \frac{\sigma_e}{K_e}\right) \cdot R_{in}^2 \cdot \left[\left(\frac{R_{out}}{R_{in}}\right)^2 - 2 \cdot \ln\left(\frac{R_{out}}{R_{in}}\right) - 1\right] + U_z B_m R_{in} \ln\left(\frac{R_{out}}{R_{in}}\right) \quad (61)$$

The generator voltage is controlled by the space charge fraction,

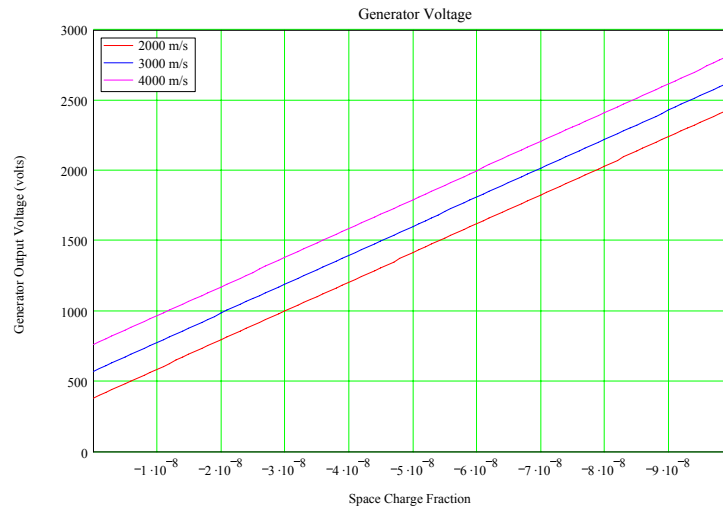


Figure 10 Generator Output Voltage

The maximum magnetic field can be determined from the load voltage equation,

$$B_m = \frac{\left[1 + 2 \cdot \ln\left(\frac{R_{out}}{R_{in}}\right) - \left(\frac{R_{out}}{R_{in}}\right)^2 \right] \cdot \left(\frac{\delta}{4} \cdot \frac{\sigma \epsilon}{\epsilon_0 \cdot K_e} \cdot R_{in} \right) + \frac{V_{load}}{R_{in}}}{U_z \cdot \ln\left(\frac{R_{out}}{R_{in}}\right)} \quad (62)$$

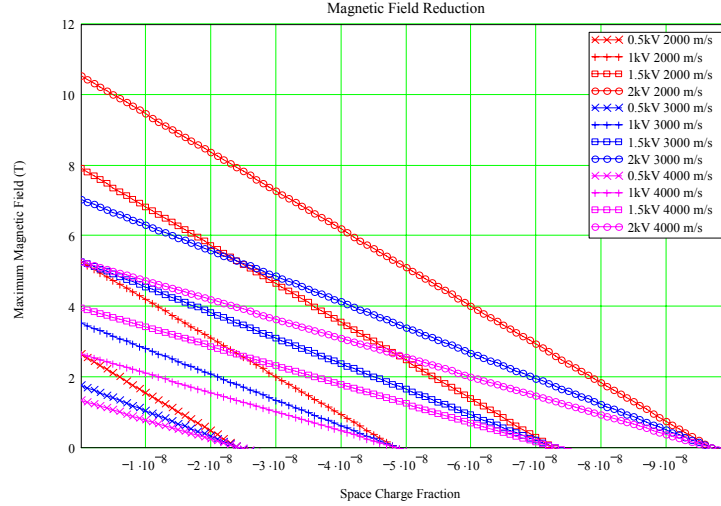


Figure 11 Magnetic Field can be reduced as Space Charge changes

The magnet current is determined using the definition of the maximum magnetic field

$$B_m = \frac{\mu_0 \cdot N \cdot I}{2 \cdot \pi \cdot R_{in}} \quad (63)$$

Solving for current and substituting the value for the maximum magnetic field, the magnet current becomes

$$I = \frac{2\pi}{\mu_0} \cdot \frac{R_{in}}{N} \cdot \frac{\left[1 + 2 \cdot \ln\left(\frac{R_{out}}{R_{in}}\right) - \left(\frac{R_{out}}{R_{in}}\right)^2 \right] \cdot \left(\frac{\delta}{4} \cdot \frac{\sigma \epsilon}{\epsilon_0 \cdot K_e} \cdot R_{in} \right) + \frac{V_{load}}{R_{in}}}{U_z \cdot \ln\left(\frac{R_{out}}{R_{in}}\right)} \quad (64)$$

The magnet current needed decreases as space charge fraction increases,

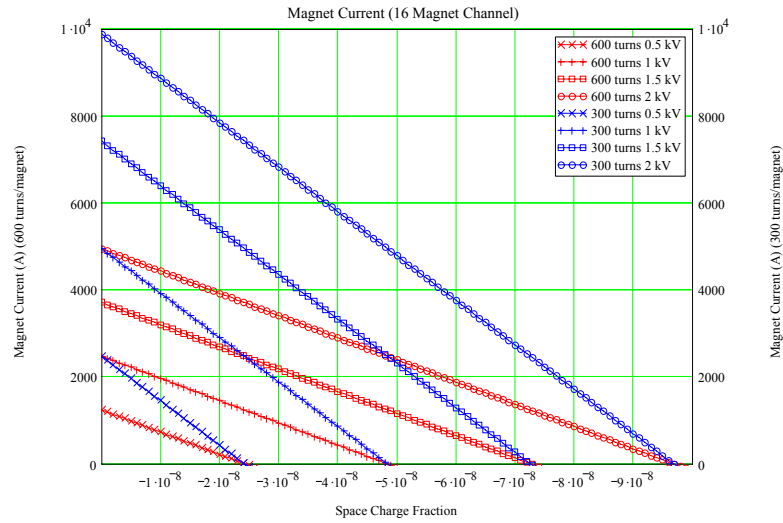


Figure 12 Magnet Current per Magnet varies with Space Charge

The space charge fraction can also be determined from the load voltage equation,

$$\delta = 4 \cdot \epsilon_0 \cdot \frac{K_e}{\sigma e} \cdot \frac{U_z B_m \ln\left(\frac{R_{out}}{R_{in}}\right) - \frac{V_{load}}{R_{in}}}{R_{in} \cdot \left[1 + 2 \cdot \ln\left(\frac{R_{out}}{R_{in}}\right) - \left(\frac{R_{out}}{R_{in}}\right)^2 \right]} \quad (65)$$

The output voltage and magnetic field can be regulated by space charge fraction,

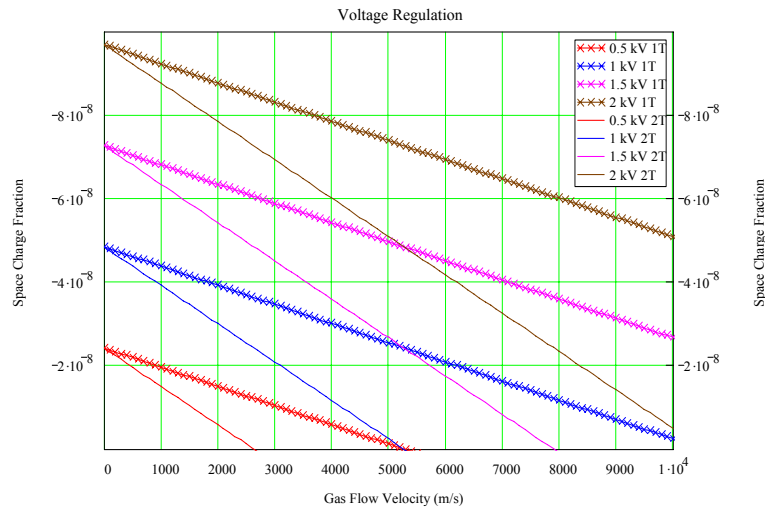


Figure 13 Voltage Regulation using Space Charge

The space charge current is determined by the equation $I_s = \delta \cdot (\sigma \epsilon / K_e) \cdot U_z \cdot \pi (R_{out}^2 - R_{in}^2)$

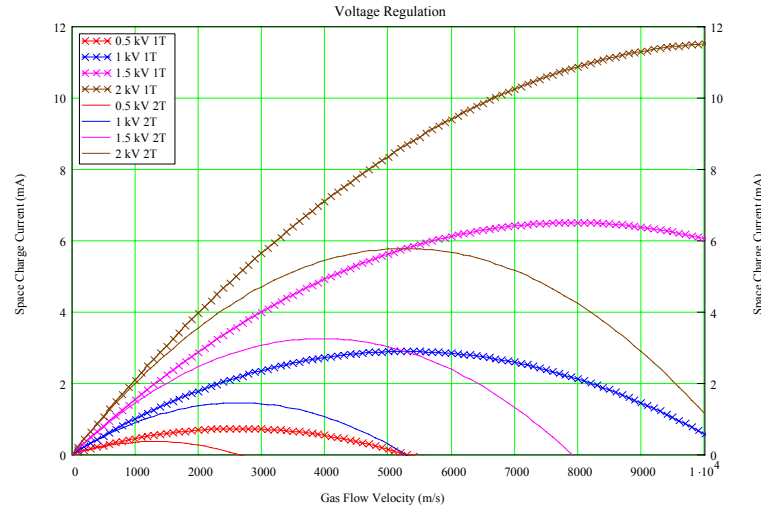


Figure 14 Space Charge Current regulates Voltage

The radial electric field in the channel with non-zero electrode surface charge

$$E_{total}(r) = \frac{1}{2} \cdot \left(2 \cdot \frac{r}{R_{in}} - \frac{R_{in}}{r} \right) \cdot \frac{\Sigma}{\epsilon_0} + \frac{1}{2} \cdot \frac{\delta}{\epsilon_0} \cdot \frac{\sigma \epsilon}{K_e} \cdot R_{in} \cdot \left(\frac{r}{R_{in}} - \frac{R_{in}}{r} \right) + U_z B_m \frac{R_{in}}{r} \quad (66)$$

The total electric field with the inner electrode grounded,

$$E_{total}(r) = \frac{1}{2} \cdot \frac{\delta}{\epsilon_0} \cdot \frac{\sigma \epsilon}{K_e} \cdot R_{in} \cdot \left(\frac{r}{R_{in}} - \frac{R_{in}}{r} \right) + U_z B_m \frac{R_{in}}{r} \quad (67)$$

The electric field at the outer electrode as space charge fraction changes,

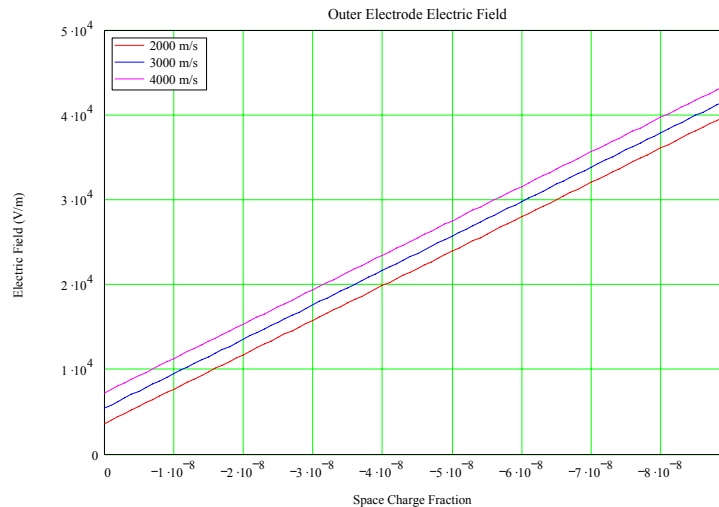


Figure 15 Generator Electric Field at Outer Electrode Surface

To determine the relationship for δ with a constant power density. Starting from the Faraday power density

$$Pd = -(U_z B \theta - E_r) \cdot [(1 + \delta) \cdot U_z B \theta - E_r] \cdot \sigma_e \quad (68)$$

We will define the term E_d so that $E_r = \delta E_d$

$$Pd = -(U_z B \theta - \delta \cdot E_d) \cdot [(1 + \delta) \cdot U_z B \theta - \delta \cdot E_d] \cdot \sigma_e \quad (69)$$

The result is,

$$Pd = \left[(U_z B \theta \cdot E_d - E_d^2) \cdot \delta^2 + (-U_z^2 \cdot B \theta^2 + 2 \cdot U_z B \theta \cdot E_d) \cdot \delta - U_z^2 \cdot B \theta^2 \right] \cdot \sigma_e \quad (70)$$

The terms in parentheses can be defined as

$$Pd = (A1 \cdot \delta^2 + B1 \cdot \delta - C1) \cdot \sigma_e \quad (71)$$

$$A1 = E_d \cdot (U_z B \theta - E_d) \quad ; B1 = -U_z B \theta \cdot (U_z B \theta - 2 \cdot E_d) \quad ; C1 = (U_z B \theta)^2$$

the solutions for space charge fractions in Equ. 67 are,

$$\delta_p = \frac{-B1}{2 \cdot A1} + \left[\frac{1}{4} \cdot \left(\frac{B1}{A1} \right)^2 + \frac{1}{A1} \cdot \frac{Pd}{\sigma_e} + \frac{C1}{A1} \right]^{\frac{1}{2}} \quad (72)$$

$$\delta_n = \frac{-B1}{2A1} - \left[\frac{1}{4} \cdot \left(\frac{B1}{A1} \right)^2 + \frac{1}{A1} \cdot \frac{Pd}{\sigma_e} + \frac{C1}{A1} \right]^{\frac{1}{2}}$$

The space charge fraction for constant output power,

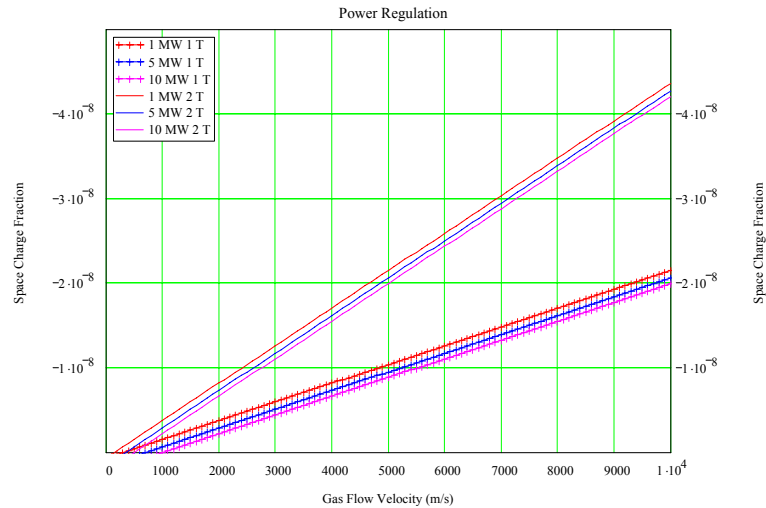


Figure 16 Power Regulation with Space Charge Changes

The space charge current for constant output power

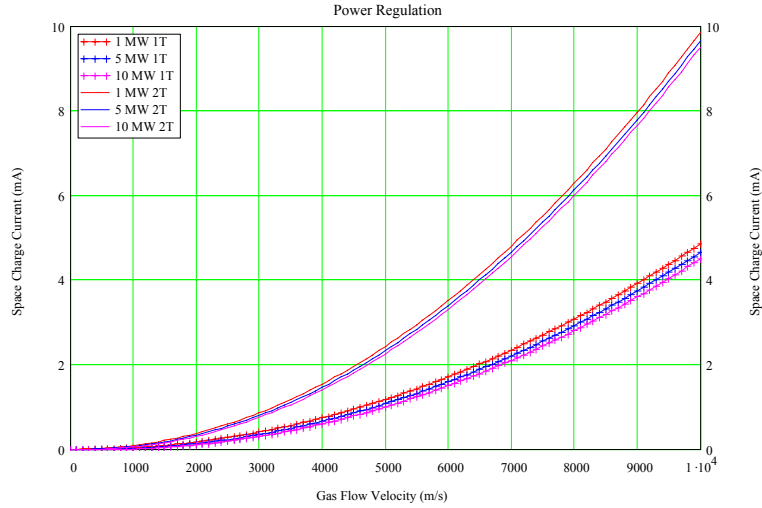


Figure 17 Power Regulation as Space Charge Current changes with Gas Flow Velocity

B. Generator Efficiency

The local efficiency η_e is defined by the ratio of electrical power density to mechanical power density

$$\eta_e = \frac{|Pd|}{|\vec{U} \cdot \vec{f}|} \quad (73)$$

Since we know the electrical power density, we now need to determine the mechanical power density $\vec{U} \cdot \vec{f}$ from the force density,

$$\vec{f} = \rho \cdot \vec{E} + \vec{J} \times \vec{B} = \delta \cdot \frac{\sigma_e}{K_e} \begin{pmatrix} E_r \\ 0 \\ 0 \end{pmatrix} + \begin{bmatrix} [(1 + \delta) \cdot U_z B_\theta - E_r] \cdot \sigma_e \\ 0 \\ (U_z \delta) \cdot \frac{\sigma_e}{K_e} \end{bmatrix} \times \begin{pmatrix} 0 \\ B_\theta \\ 0 \end{pmatrix} \quad (74)$$

This simplifies to,

$$\vec{f} = \begin{bmatrix} (E_r - U_z B_\theta) \cdot \delta \cdot \frac{\sigma_e}{K_e} \\ 0 \\ [(1 + \delta) \cdot U_z B_\theta - E_r] \cdot B_\theta \cdot \sigma_e \end{bmatrix} \quad (75)$$

The mechanical power expended on the conducting gas flowing with speed \vec{U} ,

$$\vec{U} \cdot \vec{f} = \vec{U} \cdot \left(\rho \cdot \vec{E} + \vec{J} \times \vec{B} \right) \quad (76)$$

Substituting the vectors for the velocity, electric field and magnetic field

$$\vec{U} \cdot \vec{f} = \begin{pmatrix} 0 \\ 0 \\ U_z \end{pmatrix} \cdot \begin{bmatrix} (E_r - U_z B_\theta) \cdot \delta \cdot \frac{\sigma_e}{K_e} \\ 0 \\ [(1 + \delta) \cdot U_z B_\theta - E_r] \cdot B_\theta \cdot \sigma_e \end{bmatrix} \quad (77)$$

Performing the multiplication

$$\vec{U} \cdot \vec{f} = [(1 + \delta) \cdot U_z B \theta - E_r] \cdot U_z B \theta \cdot \sigma_e \quad (78)$$

Now we can calculate the electrical efficiency

$$\eta_e = \frac{P_d}{\vec{U} \cdot \vec{f}} \quad (79)$$

Substituting the electrical power density and mechanical power density

$$\eta_e = \frac{[-(U_z B \theta - E_r) \cdot [(1 + \delta) \cdot U_z B \theta - E_r]] \cdot \sigma_e}{[(1 + \delta) \cdot U_z B \theta - E_r] \cdot U_z B \theta \cdot \sigma_e} \quad (80)$$

The electrical efficiency simplifies to,

$$\eta_e = \frac{-U_z B \theta + E_r}{U_z B \theta} \quad (81)$$

Applying the space charge electric field and the magnetic induced electric field, the electrical efficiency become,

$$\eta_e = \frac{1}{2} \cdot \frac{\delta}{\epsilon_0} \cdot \frac{\sigma_e}{K_e} \cdot \frac{R_{out}}{U_z B m} \cdot \left(\frac{R_{out}}{R_{in}} - \frac{R_{in}}{R_{out}} \right) - 1 \quad (82)$$

Space charge fractions for a constant efficiency

$$\delta = 2\epsilon_0 \cdot \frac{K_e}{\sigma_e} \cdot \frac{U_z B m}{R_{in}} \cdot \left[\frac{\eta_e + 1}{\left(\frac{R_{out}}{R_{in}} \right)^2 - 1} \right] \quad (83)$$

The space charge fraction for a constant generator electrical efficiency is shown in Fig 17.

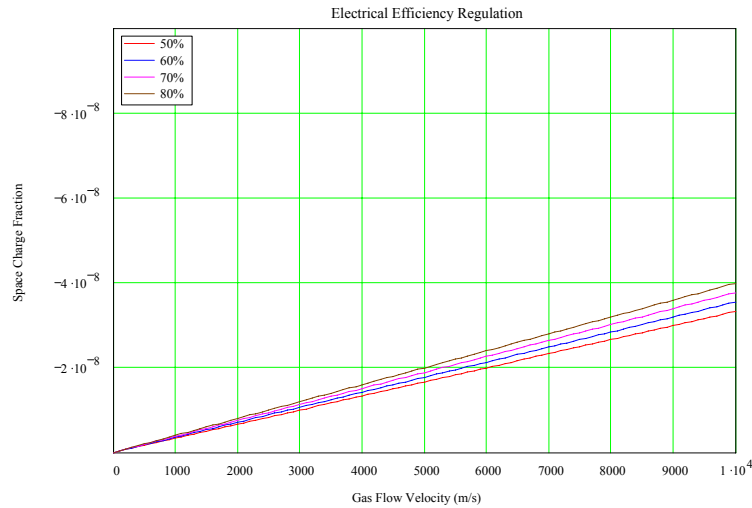


Figure 18 Electrical Efficiency Regulation as Space Charge Fraction

The space charge current for a constant generator electrical efficiency

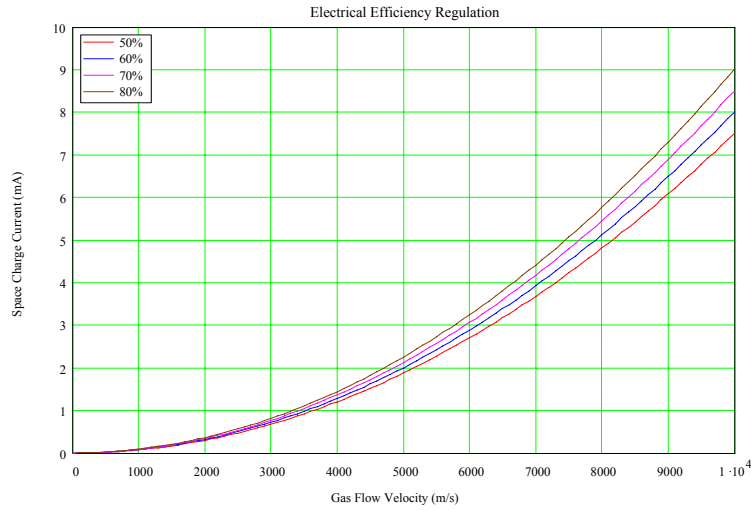


Figure 19 Electrical Efficiency Regulation with Space Charge Current

Local efficiency for constant load voltage and magnetic field

$$\delta = 4 \cdot \epsilon_0 \cdot \frac{K_e}{\sigma_e} \cdot \frac{U_z \cdot B_m \ln\left(\frac{R_{out}}{R_{in}}\right) - \frac{V_{load}}{R_{in}}}{R_{in} \left[1 + 2 \cdot \ln\left(\frac{R_{out}}{R_{in}}\right) - \left(\frac{R_{out}}{R_{in}}\right)^2 \right]} \quad (84)$$

The local or electrical efficiency is the only efficiency directly affected by changes in the electromagnetic fields. All other efficiencies are primarily affected by thermodynamic properties and only indirectly by the electrical properties through the dependence on the local efficiency.

The isentropic efficiency depends on the local efficiency,

$$\eta_p = \frac{\eta_e}{1 + \left(\frac{\gamma - 1}{2}\right) \cdot \left(\frac{U_z}{C_m}\right)^2 \cdot (1 - \eta_e)} \quad (85)$$

The total generator efficiency in turn is calculated from the isentropic efficiency,

$$\eta_g = \frac{\frac{\eta_p \cdot (\gamma - 1)}{1 - (1 - R_p)^\gamma}}{\frac{\gamma - 1}{1 - (1 - R_p)^\gamma}} \quad (86)$$

The generator efficiency depends the thermodynamic cycle properties of the generator, specifically the output to input pressure ratio (R_p) and the specific heat ratio ($\gamma = C_p/C_v$).

The space charge dependence of the generator efficiency is determined by solving Eq 76 for η_p ,

$$\eta_p = \frac{\ln\left(-\eta_g \cdot e^{-\frac{-\ln(R_p) \cdot \frac{\gamma - 1}{\gamma}}}{\eta_g + e^{-\frac{-\ln(R_p) \cdot \frac{\gamma - 1}{\gamma}}}}\right) \cdot \gamma + \ln(R_p) \cdot \gamma - \ln(R_p)}{\ln(R_p) \cdot (\gamma - 1)} \quad (87)$$

In turn we solve Eq. 75 for η_e ,

$$\eta_e = \eta_p \cdot \frac{(\gamma - 1) \cdot \left(\frac{U_z}{C_m}\right)^2 + 2}{(\gamma - 1) \cdot \left(\frac{U_z}{C_m}\right)^2 \cdot \eta_p + 2} \quad (88)$$

This is substituted into

$$\delta = 2\epsilon_0 \cdot \frac{K_e}{\sigma_e} \cdot \frac{U_z \cdot B_m}{R_{in}} \cdot \left[\frac{\eta_e + 1}{\left(\frac{R_{out}}{R_{in}}\right)^2 - 1} \right] \quad (89)$$

The plot of space charge fraction for a constant generator electrical efficiency

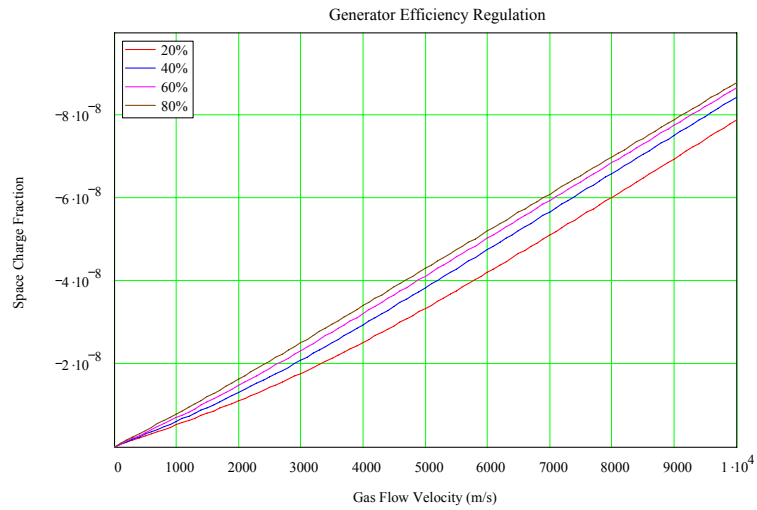


Figure 20 Generator Efficiency with Space Charge Fraction

The plot of space charge current for a constant generator electrical efficiency,

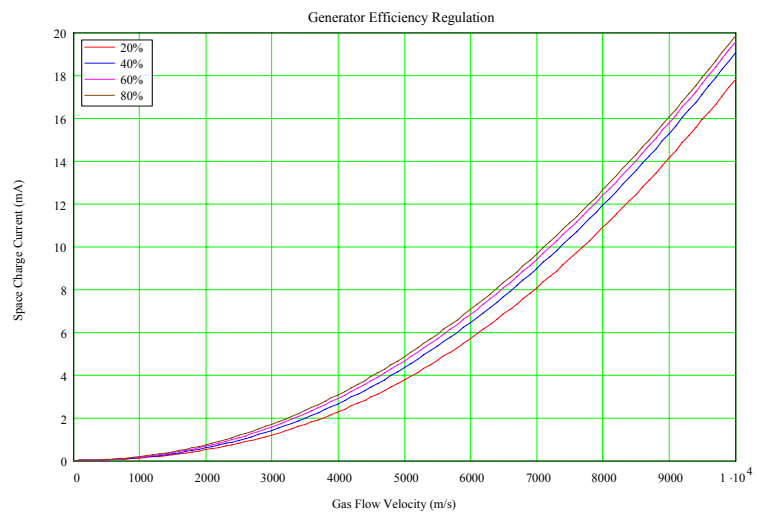


Figure 21 Generator Efficiency dependency on Space Charge Current

C. Internal Pressure Drop and Enthalpy Extraction of Generator

The axial force density for the Faraday generator is,

$$f_z = [(\delta + 1) \cdot U_z B\theta - E_r] \cdot B\theta \cdot \sigma_e \quad (90)$$

Using the minimum conductivity for the Faraday generator

$$\sigma_e = \frac{-Pd}{(B\theta \cdot U_z - E_r) \cdot [(1 + \delta) \cdot (U_z B\theta) - E_r]} \quad (91)$$

The axial force density becomes

$$f_z = [(\delta + 1) \cdot U_z B\theta - E_r] \cdot B\theta \cdot \frac{-Pd}{(B\theta \cdot U_z - E_r) \cdot [(1 + \delta) \cdot (U_z B\theta) - E_r]} \quad (92)$$

Simplifying the equation

$$f_z = Pd \cdot \frac{B\theta}{E_r - U_z B\theta} \quad (93)$$

The axial pressure drop is calculated from the integral of the force density over the length of the generator,

$$\Delta P_z = \int_0^L Pd \cdot \frac{B\theta}{E_r - U_z B\theta} dz \quad (94)$$

The integral becomes

$$\Delta P_z = Pd \cdot \frac{B\theta}{E_r - U_z B\theta} \cdot L \quad (95)$$

Using the value for the electrical efficiency

$$U_z \eta_e = \frac{E_r - U_z B\theta}{B\theta} \quad (96)$$

The axial pressure drop becomes

$$\Delta P_z = \frac{Pd}{\eta_e} \cdot \frac{L}{U_z} \quad (97)$$

The electrical efficiency can be written in terms of the constant pressure drop

$$\delta = 2\epsilon_0 \cdot \frac{K_e}{\sigma_e} \cdot \frac{U_z B_m}{R_{in}} \cdot \left[\frac{\frac{Pd}{U_z} \cdot \frac{L}{\Delta P_z} + 1}{\left(\frac{R_{out}}{R_{in}} \right)^2 - 1} \right] \quad (98)$$

The plot of generator pressure drop with space charge fraction

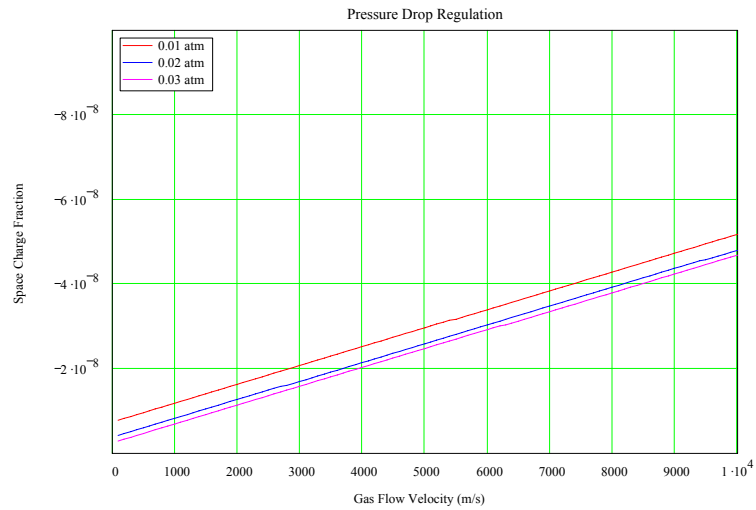


Figure 22 Pressure Drop Regulation with Space Charge

The plot of space charge current for constant generator pressure drop,

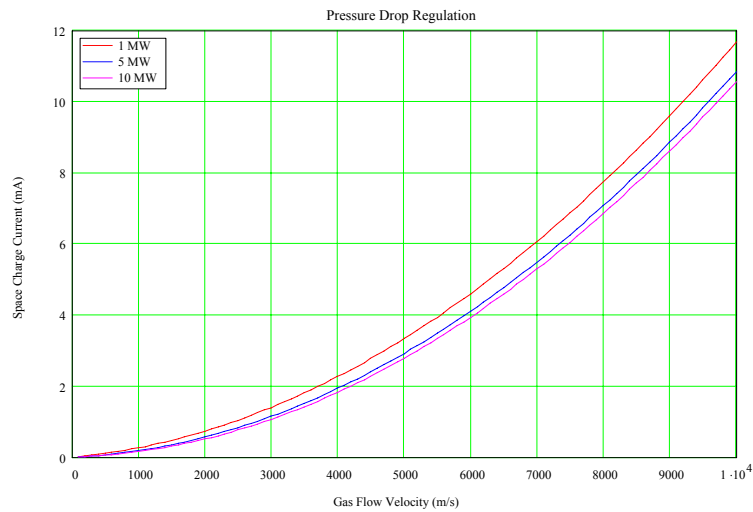


Figure 23 Pressure Drop Regulation with Space Charge Current

The reduction of thrust caused by the generator is

$$Th = Area \cdot \Delta Pz \tag{99}$$

Space charge fraction for constant thrust reduction

$$\delta = 2\epsilon_0 \cdot \frac{K_e}{\sigma_e} \cdot \frac{U_z B_m}{R_{in}} \cdot \left[\frac{\frac{P_{wr}}{U_z} \cdot \frac{1}{Th} + 1}{\left(\frac{R_{out}}{R_{in}}\right)^2 - 1} \right] \tag{100}$$

The plot of constant reduction of thrust from the generator is shown in Fig. 24.

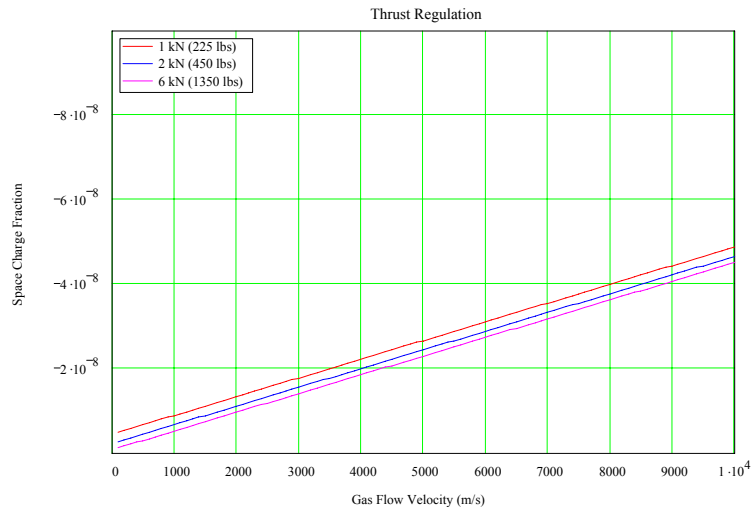


Figure 24 Thrust Reduction Regulation

The space charge current for a constant generator thrust reduction,

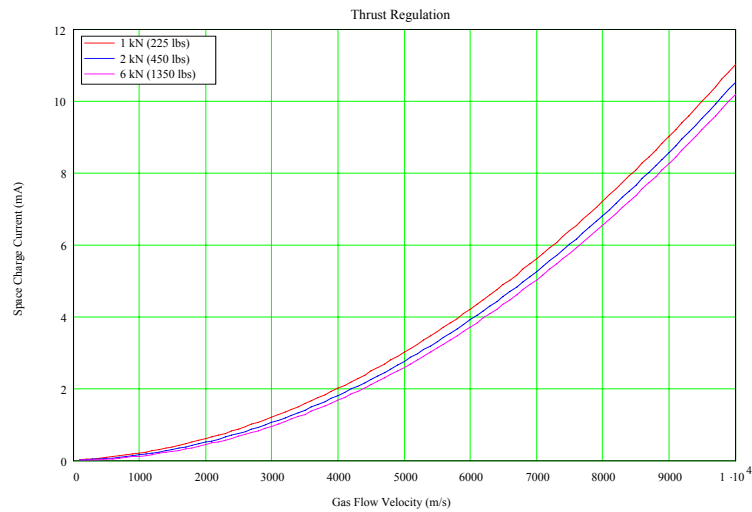


Figure 25 Thrust Reduction Regulation with Space Charge Current

The generator enthalpy drop is determined by the equation

$$h = R_{\text{gas}} \cdot \frac{T_{\text{in}}}{P_{\text{in}}} \cdot \left(\frac{P_d}{\eta_e} \cdot \frac{L}{U_z} \right) \quad (101)$$

The main byproducts of scramjet combustion have essentially the same thermodynamic properties of air, so using the universal gas constant for air ($R_{\text{gas}}(\text{air}) = 287.05 \text{ Joule/Kg/K}$) as well as the heat capacity for air ($C_p(\text{air}) = 1005 \text{ J/Kg/K}$) are accurate enough to calculation of extracted enthalpy.

The electrical efficiency for a constant enthalpy from Equ.,

$$\eta_e = R_{gas} \cdot T_{in} \cdot Pd \cdot \frac{L}{h \cdot Pin \cdot Uz} \quad (102)$$

Space charge fraction for a constant enthalpy becomes,

$$\delta = 2\epsilon_0 \cdot \frac{Ke}{\sigma_e} \cdot \frac{Uz \cdot Bm}{Rin} \cdot \left[\frac{R_{gas} \cdot T_{in} \cdot Pd \cdot \frac{L}{h \cdot Pin \cdot Uz} + 1}{\left(\frac{R_{out}}{R_{in}}\right)^2 - 1} \right] \quad (103)$$

The constant enthalpy is shown in Fig 26.

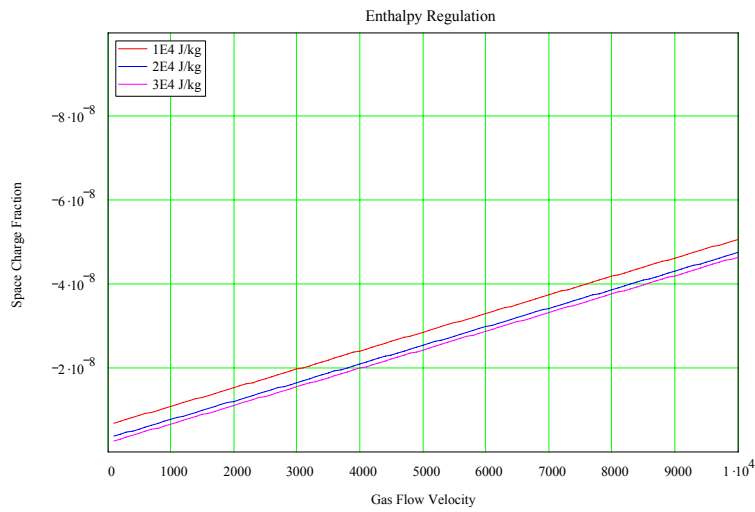


Figure 26 Enthalpy Regulation

The space charge current for a constant generator enthalpy is shown here.

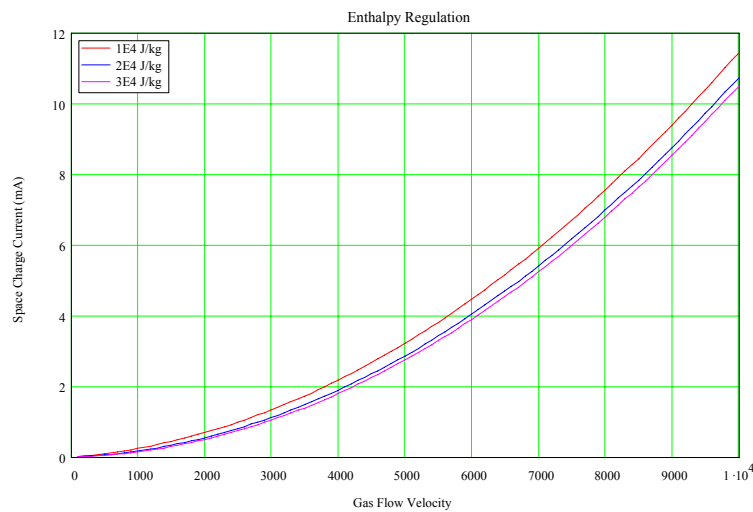


Figure 27 Enthalpy Regulation with Space Charge Current

D. Electromagnetic Reynolds Number

The Reynolds' number is generally interpreted as the ability of the fluid dynamics to modify the electromagnetic field. The definition of the electromagnetic Reynolds' number is the ratio of extracted electrical energy to total stored energy in the electromagnetic field,

$$R = \frac{u}{ub} \quad (104)$$

The electrical energy density extracted from the gas flow is,

$$u = \frac{1}{\eta e} \cdot \frac{Pd}{Uz} \cdot L \quad (105)$$

The energy density stored in the electromagnetic field is,

$$ub = \frac{1}{2} \cdot \frac{B\theta(Rout)^2}{\mu_0} + \frac{1}{2} \cdot \epsilon_0 Er(Rout)^2 + \frac{1}{2} \cdot \epsilon_0 Ez(Rout)^2 \quad (106)$$

Rewriting the last two terms of the stored energy,

$$ub = \frac{1}{2} \cdot \frac{B\theta^2}{\mu_0} + \frac{1}{2} \cdot \frac{\epsilon_0 \cdot \mu_0}{\mu_0} Er(Rout)^2 + \frac{1}{2} \cdot \frac{\epsilon_0 \cdot \mu_0}{\mu_0} Ez(Rout)^2 \quad (107)$$

Permittivity and permeability are related to the speed of light ($\epsilon_0 \mu_0 = 1/c^2$)

$$ub = \frac{1}{2} \cdot \frac{B\theta(Rout)^2}{\mu_0} + \frac{1}{2} \cdot \frac{1}{\mu_0 \cdot c^2} Er(Rout)^2 + \frac{1}{2} \cdot \frac{1}{\mu_0 \cdot c^2} Ez(Rout)^2 \quad (108)$$

Substituting the values for the magnetic field and the Faraday electric field condition ($Ez = 0$)

$$ub = \frac{1}{2} \cdot \frac{\left(Bm \cdot \frac{Rin}{Rout} \right)^2}{\mu_0} + \frac{1}{2} \cdot \frac{1}{\mu_0} \cdot \left(\frac{Er(Rout)}{c} \right)^2 \quad (109)$$

Now substituting the value for the radial electric field

$$ub = \frac{1}{2} \cdot \frac{\left(Bm \cdot \frac{Rin}{Rout} \right)^2}{\mu_0} + \frac{1}{2} \cdot \frac{1}{\mu_0} \cdot \left[\left[\frac{1}{2} \cdot \delta \cdot \frac{1}{Uz \cdot Bm} \cdot \frac{\sigma e}{Ke \cdot \epsilon_0} \cdot \left(\frac{Rout}{Rin} - \frac{Rin}{Rout} \right) \right] \cdot \left(\frac{Uz}{c} \cdot Bm \right) \right]^2 \quad (110)$$

The stored energy density term can be written as,

$$ub = \left[1 + \left[\frac{1}{2} \cdot \delta \cdot \frac{1}{Uz \cdot Bm} \cdot \frac{\sigma e}{Ke \cdot \epsilon_0} \cdot \left[\left(\frac{Rout}{Rin} \right)^2 - 1 \right] \right]^2 \cdot \left(\frac{Uz}{c} \right)^2 \right] \cdot \left[\frac{1}{2} \cdot \frac{\left(Bm \cdot \frac{Rin}{Rout} \right)^2}{\mu_0} \right] \quad (111)$$

Since the velocity ratio $Uz/c \ll 1$ and the electromagnetic Reynolds' number becomes,

$$R = \frac{\frac{Pd}{\eta e} \cdot \frac{L}{Uz}}{\frac{1}{2} \cdot \frac{\left(Bm \cdot \frac{Rin}{Rout} \right)^2}{\mu_0}} \quad (112)$$

The electrical efficiency for a constant Reynolds' number

$$\eta_e = 2 \cdot Pd \cdot L \cdot Rout^2 \cdot \frac{\mu_0}{R \cdot Uz \cdot Bm^2 \cdot Rin^2} \quad (113)$$

Space charge fraction for constant Reynolds's number becomes

$$\delta = 2\epsilon_0 \cdot \frac{Ke}{\sigma e} \cdot \frac{Uz \cdot Bm}{Rin} \cdot \left[\frac{2 \cdot Pd \cdot L \cdot Rout^2 \cdot \frac{\mu_0}{R \cdot Uz \cdot Bm^2 \cdot Rin^2} + 1}{\left(\frac{Rout}{Rin}\right)^2 - 1} \right] \quad (114)$$

The space charge fraction for constant Reynold's number.

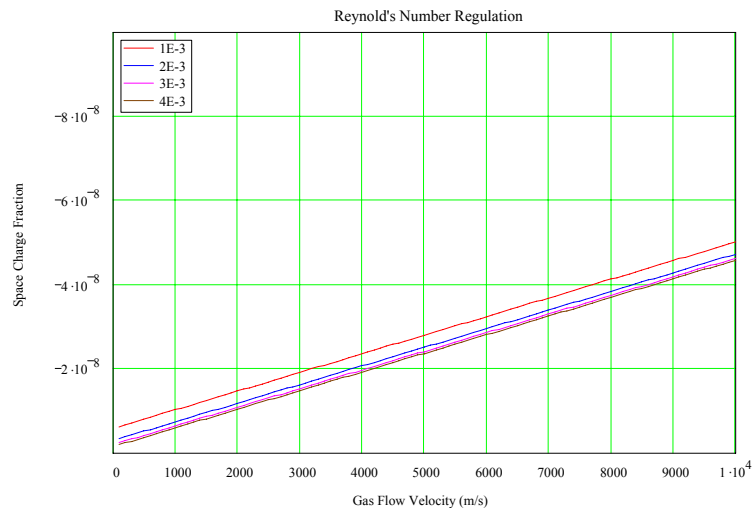


Figure 28 Reynolds' Number Regulation

The space charge current for constant Reynold's number,

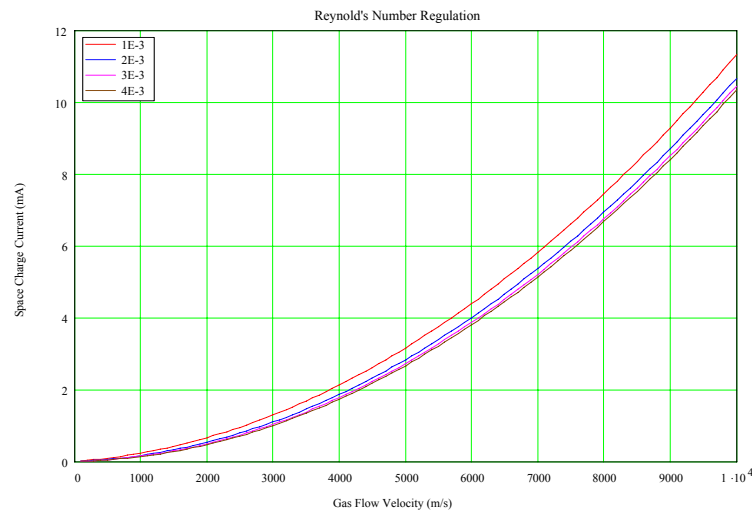


Figure 29 Reynolds' Number Regulation with Space Charge Current

E. System Weight Benefit from Eliminating the System Power Conditioner

A system weight benefit comparison can be made between using space charge regulation power supply and a full output power conditioner. The power conditioner is required when the generator voltage does not match the various load voltage. Power conditioners are notorious high mass items. The biggest limitation is the power density of converter which is typically on the order of 1kW/kg. However, for our analysis, we will assume that a large technology leap occurs in power conditioners and that the power density is 5kW/kg so that the power conditioner mass is $M_{pc} = 1000 \text{ kg}$ for a 5 MW power supply ($P = 5 \text{ MW}$). The power conditioner efficiency is assumed to be $\eta_{pc} = 98\%$ with the same large technology leaps. Assume the vehicle is moving at velocity at about Mach 6 ($U_{\text{vehicle}} = 2000 \text{ m/s}$) and the power system operates continuously over the total mission time of 4 hours ($T = 14400 \text{ s}$). This duration is reasonable if electrical power is required for MGD engine compression, plasma engine ignition, MGD surface control, etc.



Figure 30 Diffuse Electron Beam

The space charge can be provided by a diffuse electron beam to inject free electrons or a high voltage corona to inject negative ions into the gas flow. Space charging is not an attempt to increase conductivity by detaching electrons from the gas atoms. Space charging injects free electrons or attaching electrons to a small number (space charge fraction) of gas atoms. The energy cost of attaching electrons measured by the atom's electron affinity is in the range of 1-3 eV. Increasing electron conductivity through non-equilibrium ionization requires fully detaching electrons measured by the atom's ionization potential which ranges from 6-300 eV.

The power conditioner total energy cost is,

$$TE_{pc} = \frac{1}{2} \cdot M_{pc} \cdot U_{\text{vehicle}}^2 + (1 - \eta_{pc}) \cdot P \cdot T \quad (115)$$

The total energy cost to fly a full output power conditioner,

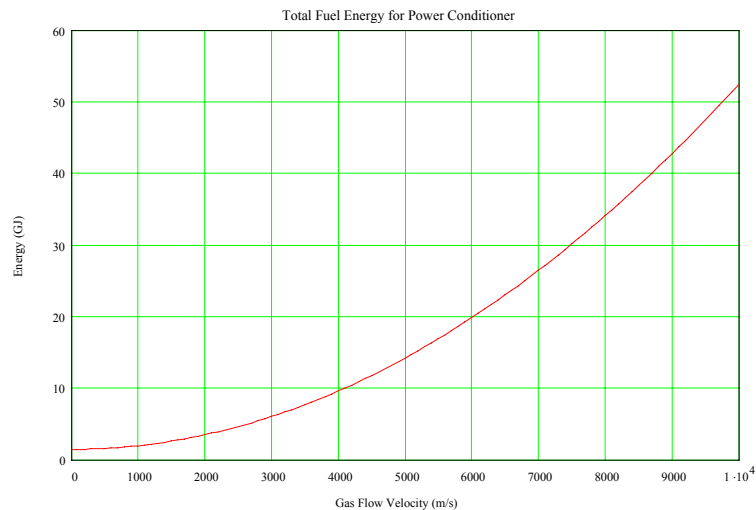


Figure 31 Total Fuel Energy Required to fly a Full Output Power Conditioner

The fuel mass required to fly a full output power conditioner

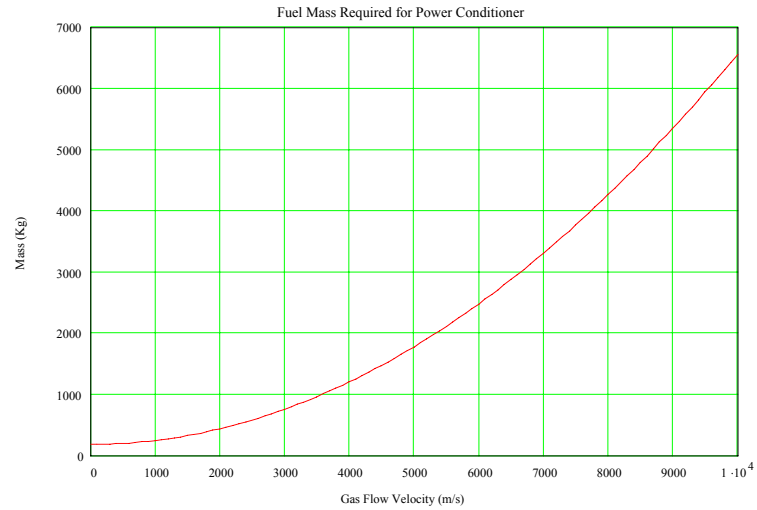


Figure 32 Fuel mass Required to fly a Full Output Power Conditioner

The minimum current for space charging is,

$$I_{eb} = \delta \cdot \frac{\sigma e \cdot U_z \cdot L}{K_e} \quad (116)$$

If the electron beam voltage is V_{eb} and the electron beam array efficiency is η_{eb} , the supply power is,

$$P_{eb} = \frac{V_{eb} \cdot I_{eb}}{\eta_{eb}} \quad (117)$$

The total energy cost of the space charger power supply is,

$$TE_{eb} = \frac{1}{2} \cdot M_{eb} \cdot U_{vehicle}^2 + P_{eb} \cdot T \quad (118)$$

The total energy cost for a space charger power supply,

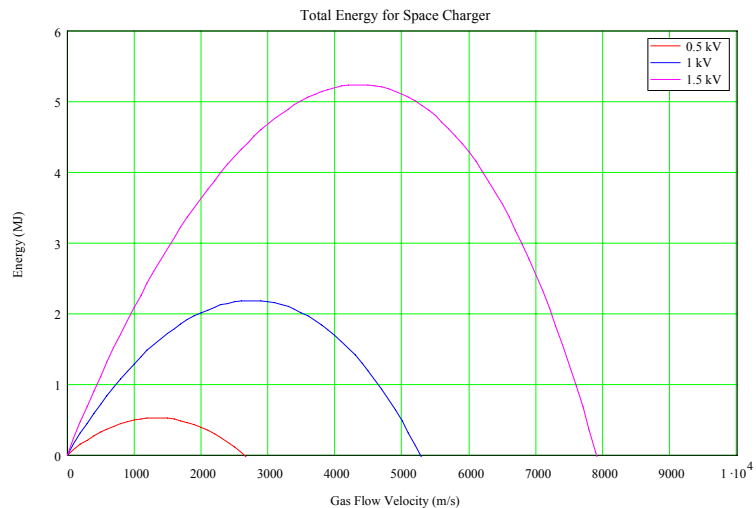


Figure 33 Total Energy Required for a Space Charger Power Supply

The fuel mass required to fly the space charger power supply,

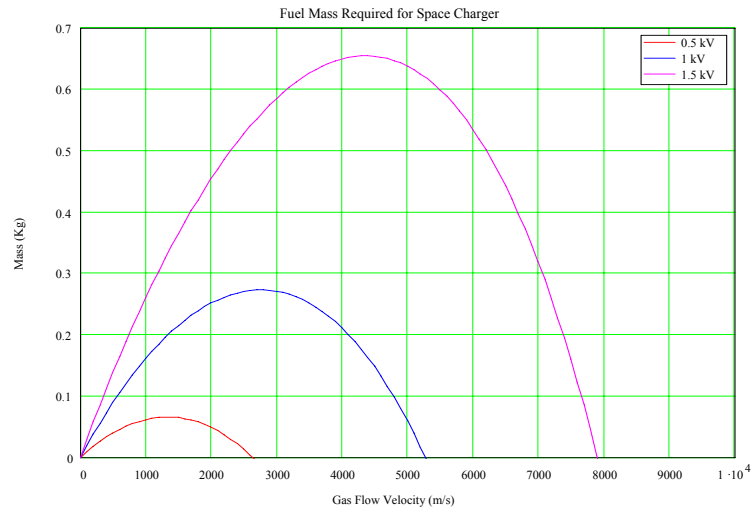


Figure 34 Fuel Mass Required for a Space Charger Power Supply

The system weight benefit is the ratio of space charger power supply energy cost to power conditioner energy cost,

$$\text{SystemBenefit} = \frac{\text{TEeb}}{\text{TEpc}} \quad (119)$$

The system benefit ratio for various generator output voltages,

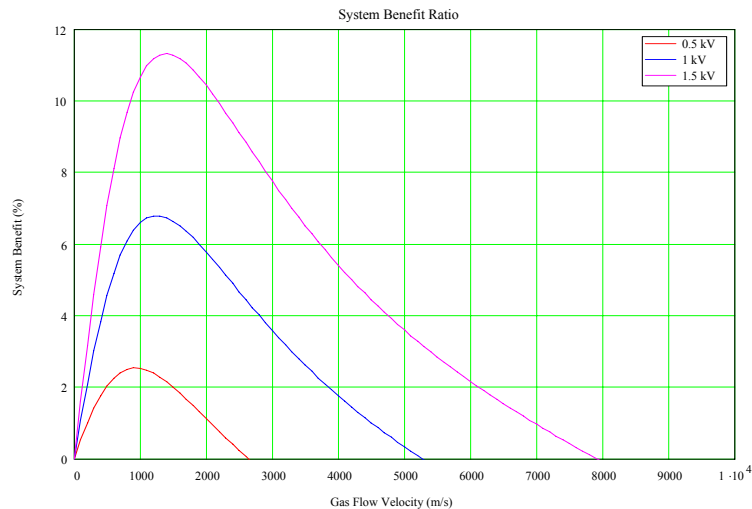


Figure 35 System Benefit Ratio

The system benefit curves show that the mass of a space charger power supply is only a small fraction of a full output power conditioner. The energy cost of lifting the mass of a power conditioner can be also measured by the mass of hydrocarbon fuel (assuming the energy density for hydrocarbons is about 40 MJ/kg) needed to lift a power conditioner. A 5MW power conditioner, based on a theoretical 5kW/kg power electronic power density, weights 1000 kg or about the same as the projected 1000 kg for a 5MW MHD generator. The full output power conditioner would require an additional 435 kg (959 lbs) of fuel to reach the 2000 m/s (4500 mi/hr or Mach 6) cruise velocity.

V. Conclusions

New methods for voltage regulation will be needed to make lightweight aerospace MHD power systems. This paper showed that space charge can be a viable method of voltage regulation for a MHD generator. Space charge would negatively alter the electric field in rectangular geometries; however, this paper shows that space charge has advantages in cylindrical generator geometries. This effect is possible because the radial space charge electric field as defined by Gauss' Law can be easily aligned with the radial electric field induced by the generator's magnet. The injected space charge can regulate the output electric field while the magnetic field remains constant. Space charge can actually reduce the amount of magnetic field needed, thereby reducing the magnet current or even reducing the number of coil windings and subsequent magnet volume and weight. Space charge voltage regulation does not require significant amounts of power or space charge current due to the low fraction of the overall electron density. The space charge regulation power supply is only a fraction of the mass of a full output power conditioner because of the low current and power required for a space charge power supply. This reduces the energy cost needed to fly a space charge power supply as compared to the energy cost needed to fly a full output power conditioner. Large technology improvements would be needed to increase the power density of full output power conditioners by a factor of 5 or 10 to make them light-weight enough to not seriously impact the weight of a MHD power system (and increase its mass fraction of a hypersonic vehicle). Replacing traditional external power conditioners with an internal method of voltage regulation represents a major technology leap in MHD generator technology that can make high power flight-weight MHD power systems practical for hypersonic vehicles.

VI. References

Books

1. Lawton and Weinberg, *Electrical Aspects of Combustion*. Clarendon Press, Oxford, 1969.
2. Messerle, Hugo, *Magnetohydrodynamic Electrical Power Generation (UNESCO Education Series)*. John Wiley & Sons, West Sussex, England, 1995.
3. Rosa, Richard, *Magnetohydrodynamic Energy Conversion*. Hemisphere Publishing Corp., New York, 1987.
4. Forrester, A. Theodore, *Large Ion Beams Fundamentals of Generation and Propagation*, John Wiley & Sons, New York, 1988.

Journals

5. Rao, K. R. and Erteza, A., "A Cylindrical Coaxial MHD Generator," *Applied Science Research*, Volume 21, Number 1, pages 427-441, January 1969.
6. Hahn, Hong-sup and Mason, E. A., "Field Dependence of Gaseous-Ion Mobility: Theoretical Tests of Approximate Formulas," *Physical Review A*, Volume 6, Number 4, October 1972
7. Robertson, Scott and Sternovsky, Zoltan, "Monte Carlo Model of Ion Mobility and Diffusion for Low and High Electric Fields," *Physical Review E*, Volume 67, October 2003.
8. Macheret, Sergey O., Shneider, Mikhail N., and Miles, Richard B., "Magnetohydrodynamic and Electrohydrodynamic Control of Hypersonic Flows of Weakly Ionized Plasmas", *AIAA Journal*, Volume 42, Number 7, July 2004.
9. Sternovsky, Zoltan, "The Effect of Ion-Neutral Collisions on the Weakly Collisional Plasma-Sheath and the Reduction of the Ion Flux to the Wall," *Plasma Sources Science and Technology*, Volume 14, Number 1, February 2005.

Proceedings

10. Krantowitz, A., "A Survey of Physical Phenomena Occurring in Flight at Extreme Speeds," *The Proceedings of the Conference on High Speed Aeronautics*, 1955
11. Meyer, Doug, et al., "Electric Auxiliary Power Unit for Shuttle Evolution", *25th Joint Propulsion Conference*, July 1989.
12. Swallow, Daniel, et al, "Results from the PAMIR-3U Pulsed Portable MHD Power System Program", *31st Intersociety Energy Conversion Conference*, August 1996.

13. Velikov, E. P., et al., "Pulsed MHD Power System 'Sakhalin' -The World Largest Propellant Fueled MHD Generator of 500 Electric Power Output," *International Conference on MHD Power Generation and High Temperature Technologies*, October 1999.
14. Miles, Richard B., et al, "High Efficiency Nonequilibrium Air Plasmas Sustained by High Energy Electrons", *International Conference on Plasma Sciences*, June 2001.
15. Thibodeaux, Rene, "Hypersonic Vehicle Electric Power System Technology", *14th International Conference on MHD Electric Power Generation and High Temperature Technologies*, May 2002.
16. Allen, Doug, et al, "Magnetohydrodynamic (MHD) Power for Directed Energy, Kinetic Energy, and High Power Surveillance Payloads on (HVEPS) Hypersonic Vehicles", *1st International Energy Conversion Engineering Conference*, August 2002.
17. Li, D, et al, "Analysis of a (HVEPS) MHD Generator", *39th Joint Propulsion Conference*, July 2003.
18. Lineberry, John T., et al, "Scramjet Driven MHD Power Demonstration – HVEPS Program", *37th Plasmadynamics and Laser Conference*, June 2006.
19. Lineberry, J. T., Begg, L., Castro, J. H. and Litchford, R. J., "Scramjet Driven MHD Power Demonstration – HVEPS Project Overview," AIAA-2006-8010, *14th AIAA/AHI International Space Planes and Hypersonic Systems and Technologies Conference*, Canberra, Australia, Nov 6-9, 2006.
20. Lineberry, John T., et al, "HVEPS Scramjet-Driven MHD Power Demonstration Test Results", *38th Plasmadynamics and Laser Conference*, June 2007.

Reports, Theses, and Individual Papers

21. AVCO Everett Research Laboratory, "High Power Density MHD Generators", AFAPL-TR-76-71, March 1976.
22. Maxwell Laboratories, "High Power Magnetohydrodynamic System", AFAPL-TR-78-51, July 1978.
23. Research Support Instruments, "MHD Power Extraction Using Nonequilibrium Plasmas In Hypersonic Flows", AFRL-PR-WP-TR-2003-2050, January 2003.
24. General Atomics, "Hypersonic Vehicle Electric Power System Technology – Delivery Order 0001 -Vehicle Power System Analysis, Tradeoff Studies, Modeling and Simulation", AFRL-PR-WP-TR-2004-2098, June 2004.
25. General Atomics, "Hypersonic Vehicle Electric Power System Technology – Delivery Order 0002 - MHD Generator Analysis, Design, Modeling and Simulation", AFRL-PR-WP-TR-2004-2097, June 2004.
26. General Atomics, "Hypersonic Vehicle Electric Power System Technology – Delivery Order 0003 - MHD Generator Magnet Analysis, Design, Modeling and Simulation", AFRL-PR-WP-TR-2004-2100, June 2004
27. General Atomics, "Hypersonic Vehicle Electric Power System Technology – Delivery Order 0004 – Hypersonic Magnetohydrodynamic Computational Fluid Dynamic Code (MHD/CFD) and Integrated Engine/Generator Test Requirements Planning", AFRL-PR-WP-TR-2004-2111, June 2004.
28. General Atomics, "Hypersonic Vehicle Electric Power System Technology – Delivery Order 0005 – Subscale Rocket Combustor Magnetohydrodynamic Generator Design", AFRL-PR-WP-TR-2006-2166, May 2006.
29. General Atomics, "Hypersonic Vehicle Electric Power System Technology – Delivery Order 0006 – Subscale Scramjet Magnetohydrodynamic Generator Design", AFRL-PR-WP-TR-2006-2072, February 2006.

Electronic Publications

30. Martinez, Marty, "General Atomics Scores Power Production First", *Space Travel.com*, URL: http://www.space-travel.com/reports/General_Atomics_Scores_Power_Production_First_999.html [cited March 15 2007]

Patents

31. B. Karlovitz, "Process for the Conversion of Energy," U. S. Patent No. 2,210,918, filed August 13, 1940.